# Hawke's Bay 3D Aquifer Mapping Project:

## Delineation of major hydrogeological units within the Heretaunga Plains from SkyTEM-derived resistivity models

February 2023
Hawkes Bay Regional Council Publication No. 5602

HAWKES BAY REGIONAL COUNCIL
TE KAUNIHERA Ā-ROHE O TE MATAU-A-MĀUI

ISSN 2703-2051 (Online)
ISSN 2703-2043 (Print)

HAWKES BAY REGIONAL COUNCIL
TE KAUNIHERA Ā-ROHE O TE MATAU-A-MĀUI

(06) 835 9200
0800 108 838
Private Bag 6006 Napier 4142
159 Dalton Street . Napier 4110

Environmental Science

# Hawke's Bay 3D Aquifer Mapping Project:

## Delineation of major hydrogeological units within the Heretaunga Plains from SkyTEM-derived resistivity models

February 2023
Hawkes Bay Regional Council Publication No. 5602

Prepared By:

GNS Science

TR Sahoo ZJ Rawlinson RL Kellett

For: Hawke's Bay Regional Council

Reviewed by:
S Harper, Hawke's Bay Regional Council
M Coble, GNS Science
C Tschritter, GNS Science



ISSN 2703-2051 (Online)
ISSN 2703-2043 (Print)

.

# Hawke's Bay 3D Aquifer Mapping Project: Delineation of major hydrogeological units within the Heretaunga Plains from SkyTEM-derived resistivity models

TR Sahoo
ZJ Rawlinson
RL Kellett

**GNS Science Consultancy Report 2022/30**
**February 2023**

GNS SCIENCE
TE PŪ AO

## DISCLAIMER

This report has been prepared by the Institute of Geological and Nuclear Sciences Limited (GNS Science) exclusively for and under contract to Hawke's Bay Regional Council. Unless otherwise agreed in writing by GNS Science, GNS Science accepts no responsibility for any use of or reliance on any contents of this report by any person other than Hawke's Bay Regional Council and shall not be liable to any person other than Hawke's Bay Regional Council, on any ground, for any loss, damage or expense arising from such use or reliance.

**Use of Data:**

Date that GNS Science can use associated data: February 2023

## BIBLIOGRAPHIC REFERENCE

Sahoo TR, Rawlinson ZJ, Kellett RL. 2023. Hawke's Bay 3D Aquifer Mapping Project: delineation of major hydrogeological units within the Heretaunga Plains from SkyTEM-derived resistivity models. Lower Hutt (NZ): GNS Science. 55 p. Consultancy Report 2022/30.

## CONTENTS



## FIGURES

## TABLES

# EXECUTIVE SUMMARY

This report focuses on the mapping of major hydrogeological units that correspond to the large-scale hydrogeological characteristics of the SkyTEM-derived resistivity models in the Heretaunga Plains as part of the Hawke's Bay 3D Aquifer Mapping Project (3DAMP).

3DAMP is a four-year initiative (2019–2023) jointly funded by the Provincial Growth Fund (PGF), Hawke's Bay Regional Council (HBRC) and GNS Science's (GNS) Groundwater Strategic Science Investment Fund (SSIF) research programme. The project applies SkyTEM technology to improve mapping and modelling of groundwater resources within the Heretaunga Plains, Ruataniwha Plains and Poukawa and Ōtāne basins. 3DAMP involves collaboration between HBRC, GNS and the Aarhus University HydroGeophysics Group (HGG).

SkyTEM is a geophysical technique that uses electromagnetic waves to investigate the shallow (~500 m) resistivity structure of the earth. SkyTEM-derived resistivity models were interpreted utilising information from a local literature review and data inventory of relevant geological, geophysical and hydrogeological information, as well as an assessment of deep, high-quality boreholes.

In total, four major hydrogeological units (HU) were manually delineated based on the resistivity models:

- HU 1 (confining unit)
- HU 2 (shallow aquifer unit)
- HU 3 (deep aquifer unit)
- HU 4 (basement unit).

These units were delineated within a defined Heretaunga model area, which extends offshore.

HU 1 (Q1 deposits) forms the major confining unit in the area and exhibits a low to moderate resistivity signature. This HU includes the clay-silt-dominated lithology of the Awatoto Member and the overlying lithologies of the Tollemache Member of the Heretaunga Formation.

HU 2 (Q1–Q5 deposits) forms the shallow aquifer unit in the area and mainly exhibits a high resistivity signature, with some minor areas of low to moderate resistivity. This HU includes the Maraekakaho Formation (Last Glacial gravels) and all terrestrial sediments of the Heretaunga Formation (Tollemache Member) that do not overlie the clay-silt-dominated sediments of the Awatoto Member, as well as Q5 sediments with a moderate to high resistivity signature.

HU 3 (Early to Middle Pleistocene deposits, including Q5–Q7 deposits) forms a deeper aquifer unit that consists of alternating layers of low and high resistivity, which are interpreted to be alternating aquifer and aquitard materials. This HU includes the penultimate glacial gravels, the last and penultimate interglacial, Brookfields Formation and Kidnappers Group sediments.

HU 4 (Paleocene to Early Pleistocene deposits) forms the hydrogeological basement unit and primarily exhibits a low resistivity signature. This HU includes various consolidated rock formations. Some groundwater resources are present within the limestone dominated areas of the Mangaheia group, which exhibit a high resistivity signature.

The datasets from this study enable a detailed 3D view of the subsurface hydrogeology of the entire survey area that was not previously possible. Spatial distributions of the hydrogeological units are largely consistent with the existing understanding of groundwater resources in the Heretaunga Plains, with additional refinements of the confining and shallow aquifer layers. The SkyTEM data in this study also improves mapping of the deep aquifer unit and the hydrogeological basement in the region.

The gridded surfaces of the boundaries between the major hydrogeological units provide valuable information that will be utilised within subsequent interpretation and modelling work as part of 3DAMP.

# 1.0 INTRODUCTION

This report focuses on the mapping of major hydrogeological units in the Heretaunga Plains using SkyTEM-derived resistivity models as part of the Hawke's Bay 3D Aquifer Mapping Project (3DAMP).

3DAMP is a four-year initiative (2019–2023) jointly funded by the Provincial Growth Fund (PGF), Hawke's Bay Regional Council (HBRC) and GNS Science's (GNS) Groundwater Strategic Science Investment Fund (SSIF) research programme. The project applies SkyTEM technology to improve mapping and modelling of groundwater resources within the Heretaunga Plains, Ruataniwha Plains and Poukawa and Ōtāne basins. 3DAMP involves collaboration between HBRC, GNS and the Aarhus University HydroGeophysics Group (HGG).

SkyTEM is a geophysical technique that uses electromagnetic waves to investigate the shallow (~500 m depth) resistivity structure of the earth. SkyTEM data were collected in the Hawke's Bay region during January/February 2020 (SkyTEM Australia Pty Ltd 2020). Using these data, resistivity models were developed for the Heretaunga Plains by Rawlinson et al. (2021). A data inventory of supporting datasets and current state of information, to support hydrogeological interpretation of these resistivity models, was developed by Tschritter et al. (2022). Kellett et al. (2022) assessed resistivity information against deep, high-quality boreholes in the area. The work presented in this report utilises models, data and information from Tschritter et al. (2022) and Kellett et al. (2022) to interpret the major hydrogeological units apparent within the SkyTEM-derived resistivity models (Rawlinson et al. 2021).

Sections 1.1 and 1.2 describe the objectives of this work and provide a brief explanation of hydrogeological interpretation using resistivity values, respectively. Section 2 summarises key information from Rawlinson et al. (2021), Tschritter et al. (2022) and Kellett et al. (2022) related to input datasets and interpretation decisions. Section 3 describes the methodology, and Section 4 presents the results of this work. Section 5 describes the digital deliverables, and Section 6 provides conclusions and recommendations.

## 1.1 Objectives

The key objective for this report is to delineate major hydrogeological units that correspond to the large-scale hydrogeological characteristics of the SkyTEM-derived resistivity models in the Heretaunga Plains. To support subsequent modelling tasks, these major hydrogeological units are required to be developed as continuous gridded surfaces throughout the study area.

Major hydrogeological unit modelling decisions (e.g. defining hydrogeological characteristics of importance) are partially informed by what the surfaces/models are going to be utilised for. Expected applications include: (1) conceptual hydrogeological modelling, (2) 3D hydrogeological modelling, (3) numerical groundwater flow and transport modelling and (4) more advanced quantitative interpretations and finer-detailed classifications within each major hydrogeological unit.

To meet these requirements, a Heretaunga model area was defined that covers both the extent of the current Heretaunga Plains numerical groundwater model (Rakowski and Knowling 2018) and extends 300 m from each SkyTEM-derived 1D resistivity model (Figure 1.1).

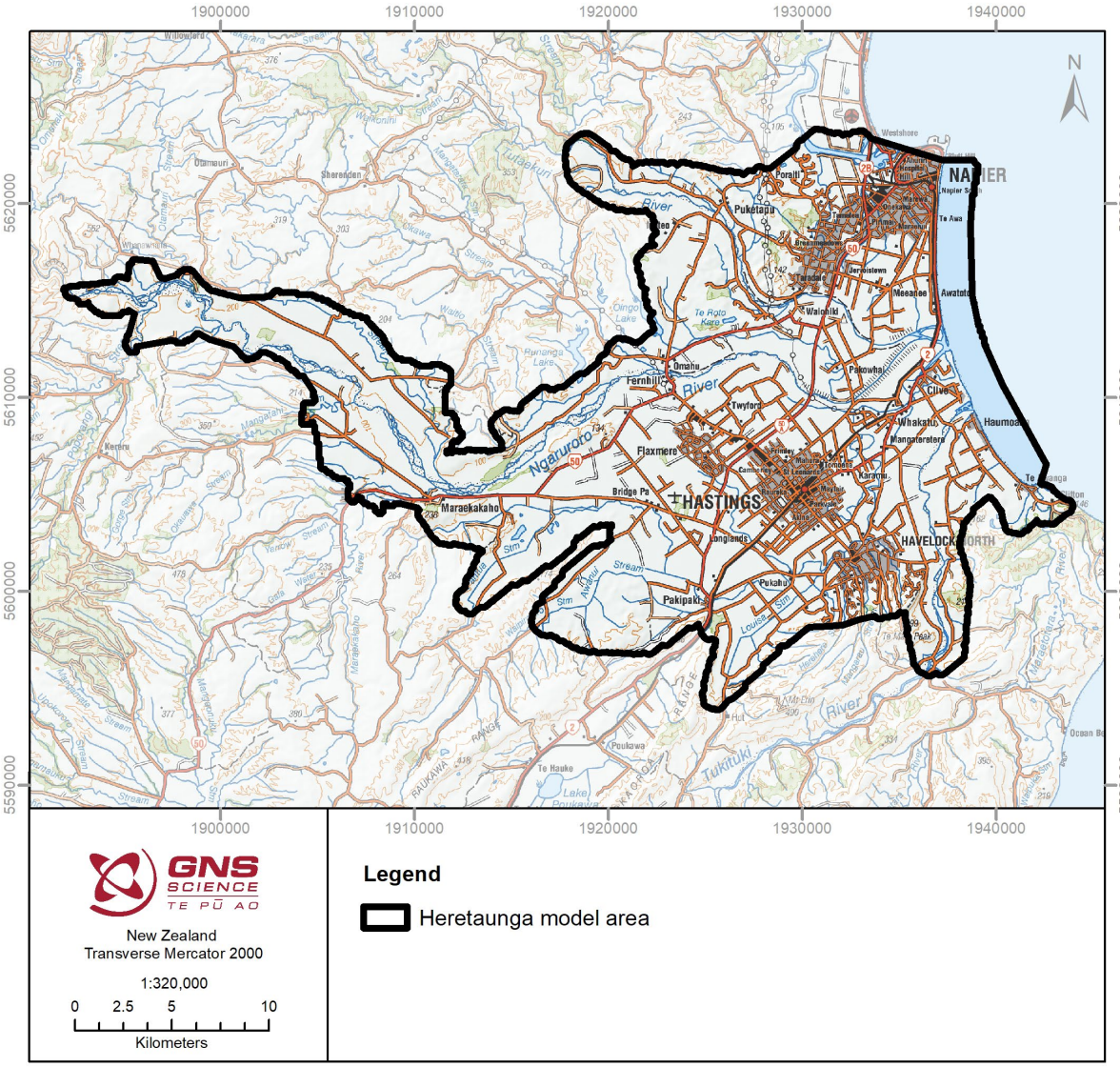


Figure 1.1 Location map of the Heretaunga Plains showing the extent of the Heretaunga model area (combined extent of the current Heretaunga Plains numerical groundwater model [Rakowski and Knowling 2018] and 300 m from each SkyTEM-derived 1D resistivity model).

## 1.2 What is Hydrogeological Interpretation?

Hydrogeological interpretation of resistivity models is a process of translating resistivity values (typically represented by the unit ohm.m or Ω·m) to categorical or numerical values of more immediate use to a hydrogeologist.

The numerical values present in a resistivity model are a function of complex relationships between porosity, permeability, grain size and sorting, mineralogical content such as clay, and fluid properties. There are no unique mathematical equations established that directly link geological material with resistivity values. Wide ranges of resistivity values have been empirically correlated to various unconsolidated and consolidated lithologies (e.g. Figure 1.2). These values will be locale-specific and may be spatially variable within a locale due to subtle geological variations (e.g. different facies or depositional processes).

Supporting local information is therefore required to interpret the resistivity models. This includes information such as surface geological maps and subsurface geological logs from drilling (see Section 2). The reliability of interpretations is therefore biased by the quality of the local

information and to areas with more information to compare to the resistivity models. A data inventory of supporting datasets and current state of information, to support hydrogeological interpretation of resistivity models within the Heretaunga Plains area, was developed by Tschritter et al. (2022), and key information from this work is summarised in Section 2.2.

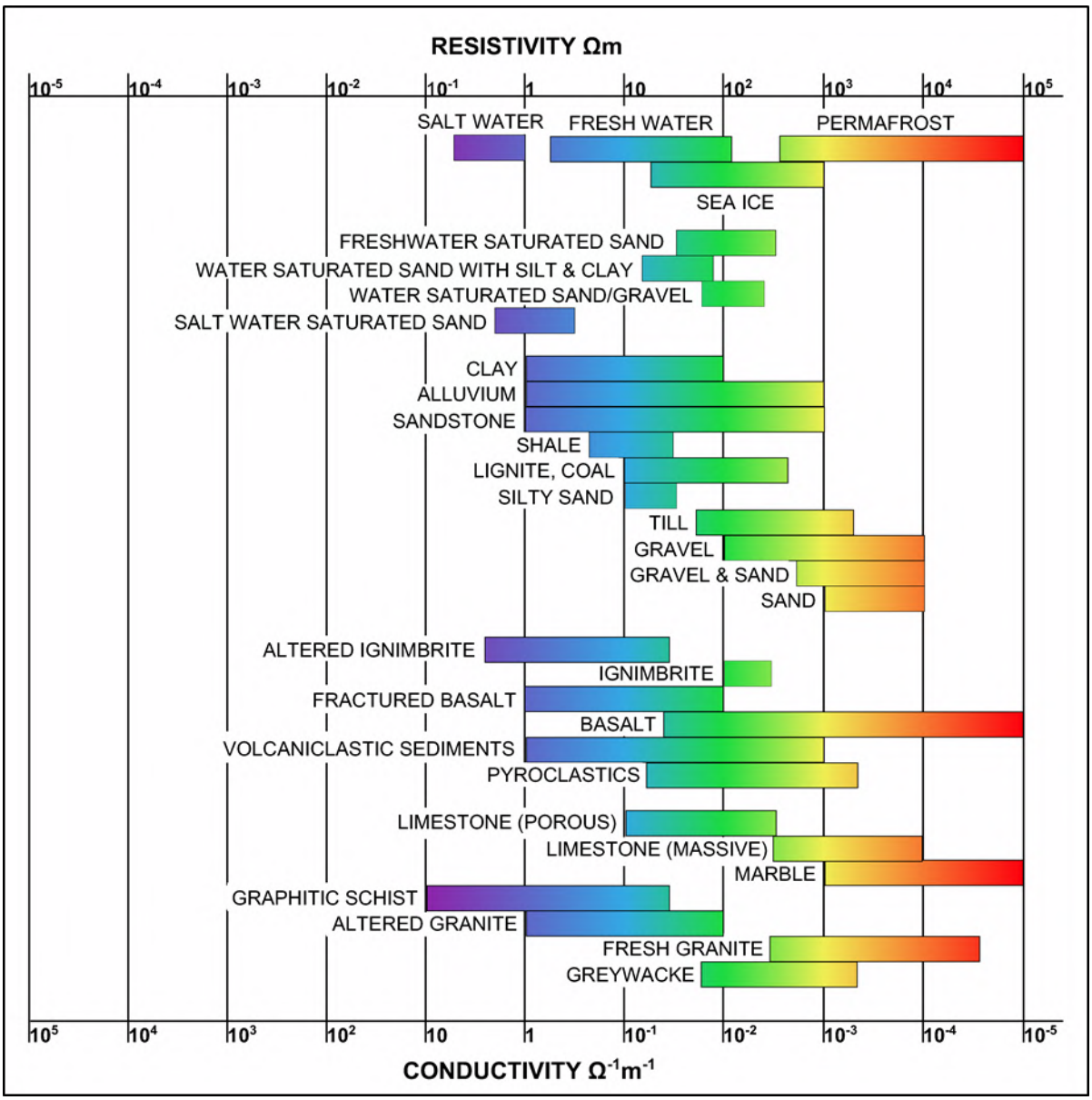


Figure 1.2 Ranges of electrical resistivity for some common lithologies measured in-situ, compiled from a variety of publications. Figure from Rawlinson (2013).

## 2.0 INPUT DATA AND INFORMATION

Input data and supporting information in this study consists of (1) SkyTEM-derived resistivity models (Rawlinson et al. 2021); (2) digital elevation model (DEM), geological data (surface geological map, borehole data, previous geological and numerical groundwater models), hydrogeological information and geophysical data (seismic reflection, DC resistivity, GroundTEM and shallow groundwater geophysical data) as summarised in Tschritter et al. (2022); and (3) assessments of deep boreholes, including the recently drilled groundwater borehole 3DAMP_Well2/17137 (Kellett et al. 2022). These datasets are briefly described below, with some key datasets and the locations of cross-sections utilised in this report shown in Figure 2.1.

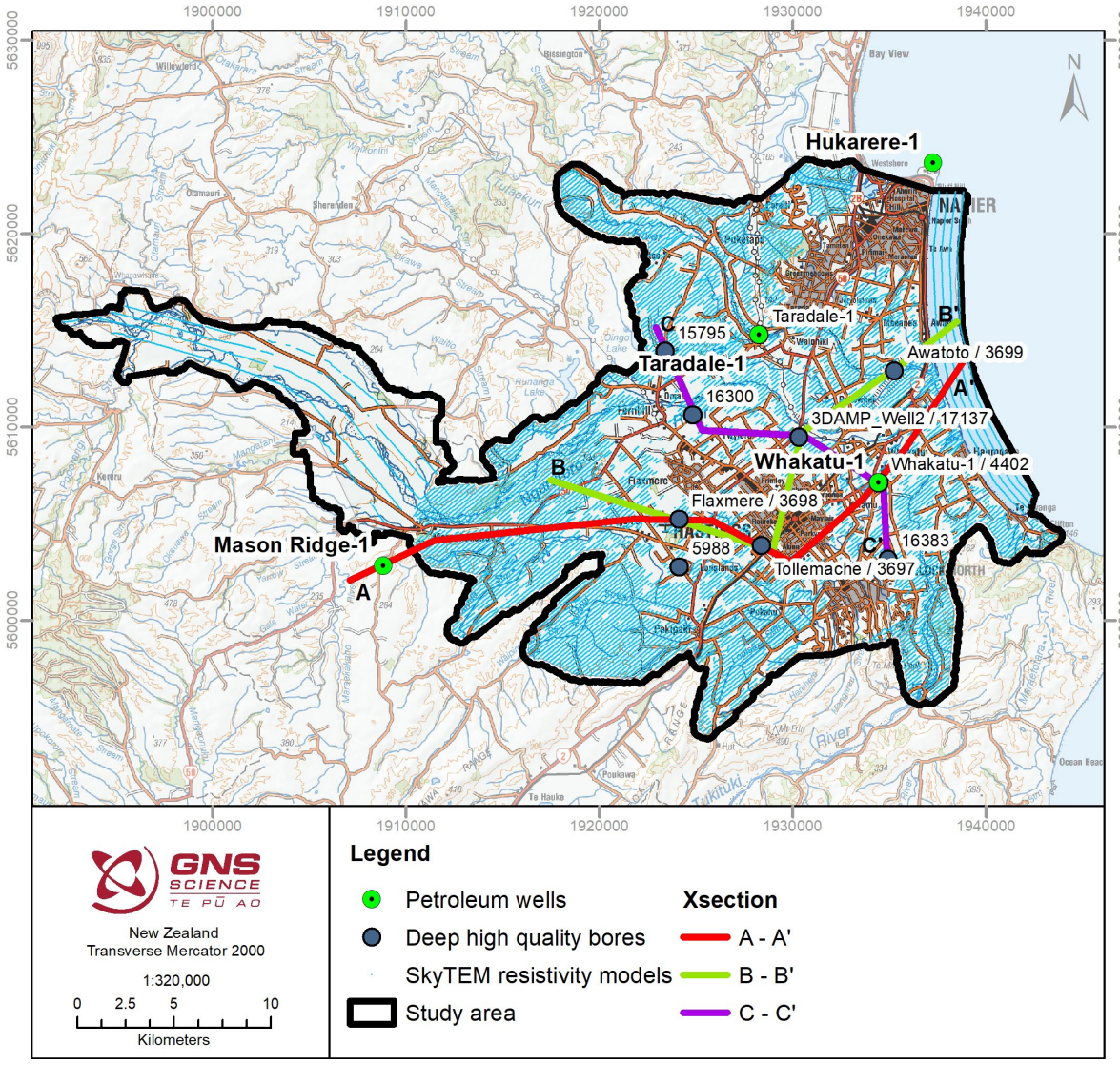


Figure 2.1 Location of SkyTEM-derived 1D resistivity models in the Heretaunga Plains. Also shown are deep, high-quality wells through which geological cross-sections were prepared.

## 2.1 Resistivity Models

The SkyTEM airborne geophysical technique is a transient (time-domain) electromagnetic method capable of investigating the shallow (usually up to 500 m deep) electrical resistivity structure of the earth (Sørensen and Auken 2004). The resistivity structure can then be interpreted in terms of geology and hydrogeology (e.g. aquifers, aquitards and aquicludes) and used to inform and improve geological and hydrogeological models. In January/February 2020, ~2610 km of SkyTEM data were collected over the Heretaunga Plains with a line spacing of ~170 m to evaluate the groundwater aquifer systems. This included four offshore lines with a ~400 m spacing and 4–5 lines in the upper Ngaruroro River valley. Details on the SkyTEM data acquisition and processing can be found in SkyTEM Australia Pty Ltd (2020), Auken et al. (2009) and Rawlinson et al. (2021).

Rawlinson et al. (2021) processed these data to remove electromagnetic noise/artefacts and to develop resistivity models. Different inversion parameters were utilised for the four offshore flight lines, and therefore separate resistivity models were provided for the onshore and offshore data. Figure 2.2 shows the extent of these models, where 1D resistivity models were developed for each data point. The resistivity models have 35 layers, and, because vertical resolution decreases with depth, the thickness of each layer increases gradually with depth. Each layer within a single 1D resistivity model is composed of a uniform resistivity value. The onshore resistivity models have layer thicknesses of 1 m in the near-surface, increasing to 59 m at depth. The offshore resistivity models have layer thicknesses of 0.1 m in the near-surface, increasing to 10.6 m at depth. As undertaking inversion modelling to develop resistivity models is a non-unique mathematical process, both smooth and sharp spatially constrained resistivity models were developed (Auken et al. 2015). The smooth model inversion provides smooth resistivity transitions both vertically and horizontally. In contrast, the sharp model inversion favours resistivity changes above a certain size and provides relatively sharp resistivity transitions.

The quality and reliability of these resistivity models depends on the SkyTEM system set-up, geological setting, flight altitude and electromagnetic noise caused by man-made structures such as powerlines. During data processing, two values for the depth of investigation (DOI) were estimated for each 1D resistivity model to highlight the limits of reliable interpretation: standard and conservative (also referred to as DOI Lower and DOI Upper, respectively). For the smooth onshore model, the standard DOI varies from 12 m to 650 m, with a mean of 276 m (Figure 2.2). For the smooth offshore model, the standard depth of investigation varies from 20 m to 72 m, with a mean of 30 m (Figure 2.2). As a guideline, resistivity structures above the DOI conservative value are considered well determined (i.e. the inversion modelling is primarily informed by the data) and resistivity structures below the DOI standard value are considered weakly determined (i.e. the inversion modelling is primarily guided by mathematical regularisation). Between the DOI conservative and the DOI standard, the resistivity model is informed by a combination of data and mathematical regularisation.

Four resistivity models in .gdb format (Firebird database format used by, for example, proprietary Aarhus Workbench Software and Geoscene3D software) were imported into GeoScene3D software (see Section 3.2) from Rawlinson et al. (2021):

- *Heretaunga_sharp_resistivitymodel_V1_2021.gdb*
- *Heretaunga_smooth_resistivitymodel_V1_2021.gdb*
- *Heretaunga_offshore_sharp_resistivitymodel_V1_2021.gdb*
- *Heretaunga_offshore_smooth_resistivitymodel_V1_2021.gdb*

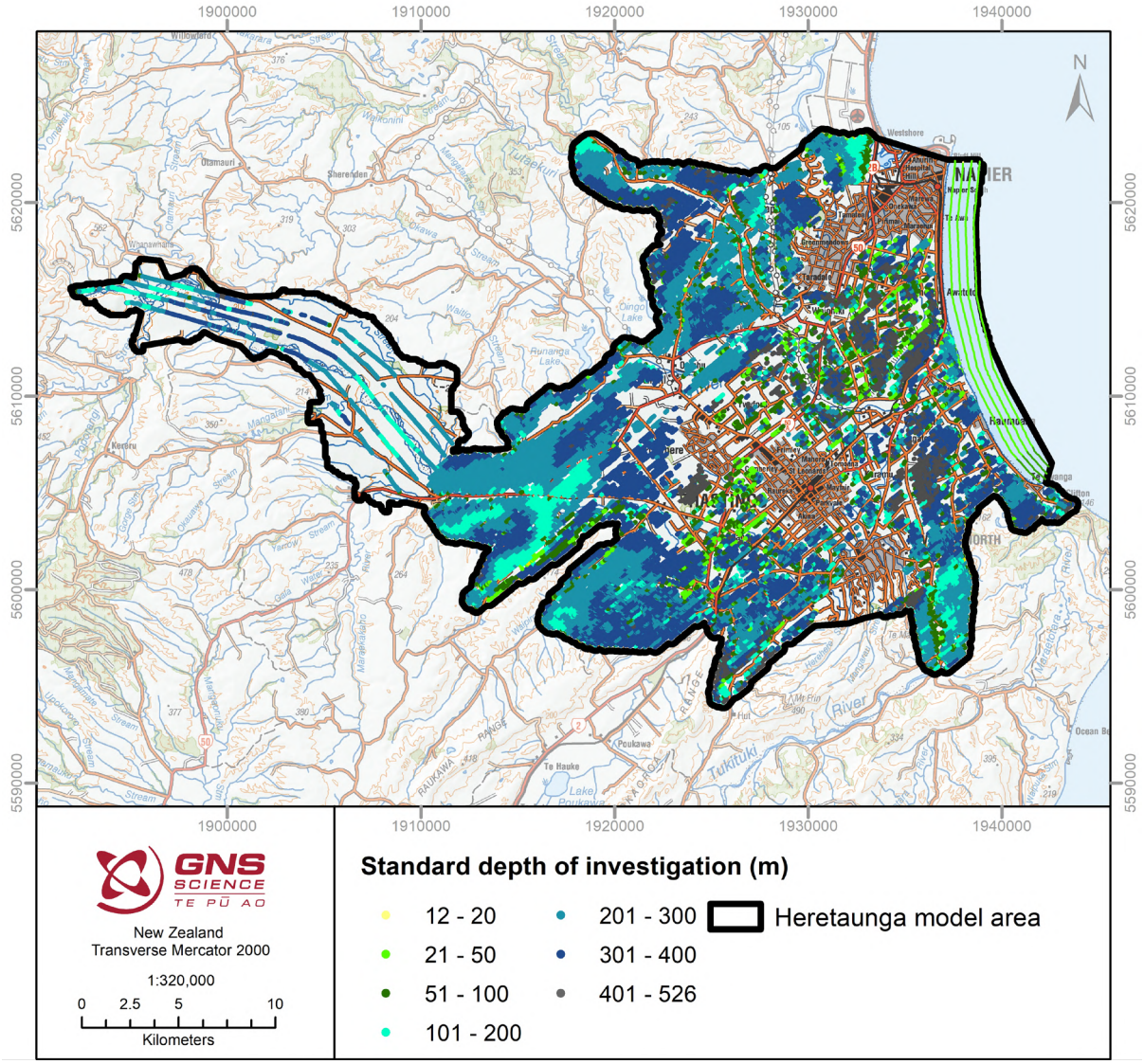


Figure 2.2 Standard depth of investigation for the smooth resistivity models.

## 2.2 Data and Model Inventory

### 2.2.1 Geology and Hydrogeology

Tschritter et al. (2022) provided a summary of the geology and hydrogeology of the area based on previous studies and models (see references therein) and provides the primary conceptual understanding and information utilised within this report. A brief summary of information from Tschritter et al. (2022) is provided below to clarify nomenclature used within this report, as well as major hydrogeological details. A comparison of different previous models with respect to the mapped layers and age are also summarised in Table 2.1 (Tschritter et al. 2022). An additional model has been added to Table 2.1 (Groundwater Numerical Model 2022) to describe current numerical modelling work being undertaken in the Heretaunga Plains as part of the Te Whakaheke o Te Wai research programme (Hemmings 2022).

The Heretaunga Plains is a fault-bounded depression, the Heretaunga Basin, that is the result of a subsiding syncline (Napier Syncline) that has been infilled by both alluvial and marine deposits that represent several glacial–interglacial cycles and associated sea-level fluctuations (Dravid and Brown 1997; Lee et al. 2011, 2014; Begg et al. 2022).

Pliocene and older sedimentary deposits are consolidated rocks and therefore considered to be the hydrogeological basement in this study. Basement rocks in the survey area are comprised of mudstone, sandstone, limestone and siltstone of Paleocene to Early Pleistocene age (Table 2.1). Pliocene Mangaheia Group sandstone, limestone and mudstone is exposed at the surface in the hill country areas north, west and south of the Heretaunga Plains (Begg et al. 2022; Lee et al. 2020). Paleocene–Eocene Mangatu Group rocks (Wansted Formation: calcareous, smectitic mudstone; and Weber Formation: glauconitic sandstone and calcareous mudstone) and Miocene Tolaga Group deposits (primarily melange and mudstone) have been mapped south of the plains. These basement rocks are interpreted to underlie the plains, but data on the basement underneath the area is sparse.

The Paleocene to Early Pleistocene basement rocks are unconformably overlain by terrestrial to marginal marine deposits of the Kidnappers Group (Early to Middle Pleistocene; Dravid and Brown 1997). These deposits primarily consist of conglomerate, sandstone and pumiceous sandstone with minor lignite, ignimbrite and paleosols. Kidnappers Group rocks have been mapped at the ground surface and have only been intersected between 75 m and 307 m depth at Whakatu-1 petroleum exploration bore drilled in 2000 (Tschritter et al. 2022). Last Glacial and interglacial (Middle to Late Pleistocene; Q5–Q7) beach deposits of the Brookfields Formation comprise sand, silt, gravel and loess deposits cropping out along hilltops at Cape Kidnappers, as well as in the southeast of the plains (Table 2.1). These deposits have also been correlated with clay, silt, gravel and peat deposits in the Awatoto and Tollemache groundwater exploration boreholes (Lee et al. 2020; Begg et al. 2022).

Maraekakaho Formation comprises thick river gravels that have been deposited across the plains during the last glaciation (Late Pleistocene; Q2–Q4) by the Ngaruroro, Tukituki and Tutaekuri rivers (Table 2.1). Due to its distinct gravel-dominated lithological composition, this formation is easily recognisable in bore logs throughout the plains. While it has been buried by Holocene deposits throughout most of the plains, Maraekakaho Formation greywacke gravel with some silt and sand beds crop out in river terraces of the Ngaruroro and Tukituki rivers (Litchfield 2003).

The Holocene (Q1) Heretaunga Formation is comprised of terrestrial and marine sediments that cover the entire plains with a thickness of ~40–50 m and consists of two members differentiated by their depositional environments: Tollemache Member and Awatoto Member (Lee et al. 2020; Tschritter et al. 2022; Table 2.1). Tollemache Member is predominantly a terrestrial deposit comprising gravel, sand, clay and silt that was deposited by the Tukituki, Ngaruroro and Tutaekuri rivers. This unit is at the ground surface throughout most of the Heretaunga Plains, but it can also be identified in the subsurface. Inland, the Tollemache Member is ~10–12 m thick, but thins towards the coast, where it interfingers with the marine deposits of the Awatoto Member. Distinct thick Holocene gravel fans associated with the Ngaruroro, Tukituki and Tutaekuri rivers, which can be identified from thick gravel deposits in bore lithological logs, may be hydraulically connected to the underlying Maraekakaho Formation (Lee et al. 2014; Begg et al. 2022). The Awatoto Member was deposited during the Holocene (Q1) marine transgression and comprises shelly marine and marginal marine silt, clay and beach gravel. The Awatoto Member was defined based on the presence of shells in the borehole data. Non-shelly marine deposits are grouped with the remainder of the Tollemache Member (Lee 2021).

This page left intentionally blank.

Table 2.1 Summary of relationships between different models and maps (Tschritter et al. 2022; Hemmings 2022). MIS = Marine Isotope Stage.

| Geological Model Unit 2014 (Lee et al. 2014) | Geological Model Unit 2022 (Begg et al. 2022) | Groundwater Numerical Model 2018 (Rakowski and Knowling 2018) | Groundwater Numerical Model 2022 (Hemmings 2022) | Depositional Climate (Dravid and Brown 1997) | Age of Interpreted Seismic Horizons (Tschritter et al. 2022) | GroundTEM Resistivity (ohm.m) (Reeves et al. 2019) | Geological Map of New Zealand at 1:250,000 (Heron 2020) | Urban Geological Map at 1:75,000 (Lee et al. 2020) |
|---|---|---|---|---|---|---|---|---|
| Q1: Ngaruroro and Tukituki fan gravels, Tukituki rivermouth gravel and Tukituki and Napier beach gravels | Heretaunga Formation (Tollemache Member), including Tutaekuri, Ngaruroro and Tukituki River gravels, and Tukituki rivermouth gravel | Layer 1 (inland) and numerically represented confining layer | Layer 1 and Layer 2 (minor and diminishing extension of river gravels to layer 5) | Post-glacial | - | ~100–2000 (gravels)<br>~10–20 (clays/silts) | MIS 1 (Holocene) river, fan, swamp, dune, reclaimed land and landslide deposits | Tollemache Member (htz, htg) |
| Q1: Holocene undifferentiated | Heretaunga Formation (Awatoto Member), including Maraenui and Haumoana gravel bars | Numerically represented confining layer | Layer 1 and Layer 2 – more dominant in Layer 2 | Post-glacial | - | ~10–20 | MIS 1 (Holocene) ocean beach and estuary deposits | Awatoto Member (hae, hab) |
| Q2–Q4: Glacial | Maraekakaho Formation | Layer 1 | Layers 3, 4, 5 | Last glacial gravels | - | ~100–2000 | MIS 4–2 Late Pleistocene to Holocene river and fan deposits | Maraekakaho Formation (ma) |
| Q5: Interglacial | Early to Middle Pleistocene | Layer 2 | Layers 6, 7, 8 | Last interglacial (‘base of gravels’ inferred from drop in resistivity) | Late Pleistocene | ~15–100 | MIS 5 (Late Pleistocene) ocean beach deposits | Brookfields Formation (bb1, bf) |
| Q6: Glacial | Early to Middle Pleistocene | Layer 2 | Layers 6, 7, 8 | Penultimate glacial gravels | - | ~15–100 | MIS 6 – MIS 2 (Middle to Late Pleistocene) fan deposits; Middle Pleistocene river deposits (mQ) | Brookfields Formation (bb2) |
| Q7: Interglacial | Early to Middle Pleistocene | Layer 2 | Layers 6, 7, 8 | Penultimate interglacial | Middle Pleistocene | ~15–100 | - | Brookfields Formation (bb2) |
| Early to Middle Quaternary | Early to Middle Pleistocene | Hydrogeological basement – no flow boundary | Hydrogeological basement – no flow boundary set when basal, flux enabled when lateral | - | Early Pleistocene | ~15–100 | Mostly Kidnappers Group | Kidnappers Group (K) |
| Basement undifferentiated | Paleocene to Early Pleistocene | Hydrogeological basement – no flow boundary | Hydrogeological basement – no flow boundary set when basal, flux enabled when lateral | Basement | - | ~4–25 | Mangatu Group, Tolaga Group, Mangaheia Group; Late Cretaceous – Early Miocene melange | Mangahaia Group, Tolgaga Group, Mangatu Group |

This page left intentionally blank.

### 2.2.2 Input Data and Relevance for SkyTEM Data Interpretation

Available hydrogeological datasets relevant to mapping major hydrogeological units using SkyTEM-derived resistivity models were previously summarised by Tschritter et al. (2022). A brief description of these datasets, uncertainties and relevance to this study is provided below.

The latest, and highest resolution, digital elevation model (DEM) that covers the SkyTEM survey area is a 5 m horizontal resolution DEM provided by HBRC (Figure 2.3; Farrier 2020). Due to file sizes and software speed, this DEM was down-sampled to 25 m resolution and converted to an ascii file for import into GeoScene3D. This DEM data helps to inform the modern-day location of structural highs and lows and the sediment dispersal pattern in the study area, as well as providing clues to understand near-surface fault movements.

The 1:250,000-scale surface geological map (Heron 2020; Figure 2.4), 1:75,000-scale surface geological map (Figure 2.5; Lee et al. 2020) and geomorphological map (Figure 2.6; Lee et al. 2020) were imported as GeoTIFF files into GeoScene3D. For reference, the 1:250,000-scale surface geological map (Heron 2020) was also displayed as main rock type (Figure 2.7). These maps provide information on outcrop lithology, geological formation / group names, age and presence of faults in the study area. This surface information provided calibration points for mapping age-equivalent layers within the subsurface using borehole and geophysical data. In areas where there is no or less SkyTEM and borehole data coverage, these maps provide major control points at the surface for mapping age-equivalent layers in the subsurface. ArcGIS shapefile polygons of geological formations were also used to refine grid boundaries at the surface.

Lithological borehole data were compiled by Tschritter et al. (2022) (Figure 2.8). All lithological intervals were imported into GeoScene3D using the main recorded lithology in each interval for colour-coding. Overall, lithological information in the upper 40 m is relatively well constrained, whereas very limited information is available below 100 m to constrain the geological and hydrogeological interpretations. The HBRC well database contains 5810 boreholes within the limits of the SkyTEM survey area, and the mean depth of the 5083 wells with recorded bore depth information was ~33 m (Tschritter et al. 2022). There are four research wells available in the survey area, among which three were drilled in 1991–1994 (Flaxmere, Tollemache and Awatoto; Dravid and Brown 1997) and one was drilled in 2021 (3DAMP_Well2; Lawrence et al. 2021). These wells provide geological and hydrogeological information of deeper units up to 256.5 m (total depth at Tollemache). Petroleum exploration wells available within or close to the SkyTEM survey area are Mason Ridge-1, Whakatu-1, Taradale-1 and Hukarere-1 (Figure 2.8); however, only Whakatu-1 provides information on the central plains area. These wells provide detailed geological, stratigraphic and petrophysical data for deeper intervals in the survey area. Information from these wells also provided ties for the seismic data interpretation (Tschritter et al. 2022). Among these wells, Whakatu-1 and Taradale-1 contain valuable information on the Quaternary geology. Wells Hukarere-1 and Mason Ridge-1 mainly intersect early Pleistocene and older sediments.

The recent 2022 3D geological model (Begg et al. 2022), developed in Leapfrog Geo 3D modelling software, provides an update of the previous 2014 3D geological model (Figure 2.9; Lee et al. 2014) for the Napier-Hastings area and is focused on the distribution of Quaternary sediments and differentiation of Holocene units (Begg et al. 2022). The updated geological model was based on a DEM, surface geological map, Land Information New Zealand 1:250,000-scale Topo250 map, radiocarbon ages (Dravid and Brown 1997), borehole lithological logs provided by HBRC, petroleum wells and seismic data interpretation (an older seismic interpretation than that presented in Tschritter et al. [2022]). Four modelled geological

unit boundaries from the updated geological model were imported into GeoScene3D as 2D grid files (ascii format; Begg et al. 2022). These boundaries represent the (1) base of the Heretaunga Formation, (2) base of the Maraekakaho Formation, (3) base of the Early to Middle Pleistocene and (4) top of the Paleocene to Early Pleistocene. The recent geological model (Begg et al. 2022) also defines two sub-units within the Heretaunga Formation: Awatoto Member and Tollemache Member. In general, the uncertainty in the interpretation of these boundaries is high in areas with a smaller number of wells. The uncertainty in interpretation is also high below ~50 m depth due to the limited number of deeper wells providing information on lithology and age information. Understanding of the regional geologic framework was used to assign boundaries in areas where borehole data were limited or of insufficient detail (for example, the inland base of the Maraekakaho Formation). Though this model does not cover the entire SkyTEM survey area, it provides a first-order understanding of the structure of the major geological units in the Paleocene–Quaternary throughout most of the study area. Additionally, to create continuous surfaces through the model area, this information was used to support surface interpretations at depths below the SkyTEM data extent. The naming of formations utilised in this report and a brief description of the model layers is provided in Table 2.2.

Seismic reflection profiles available in the SkyTEM survey area (Figure 2.10) were correlated to the petroleum wells using three key seismic markers: Late Pleistocene, Middle Pleistocene and Early Pleistocene (Tschritter et al. 2022). In general, the near-surface (top 200 m) data quality was low; however, below this depth, the structure of the different layer boundaries are well imaged in seismic sections. The Late Pleistocene sequence of interbedded gravels, sands, silts and clays occurs between the Late and Middle Pleistocene markers. The top of the Kidnappers Group is identified by the Middle Pleistocene marker. The Early Pleistocene marker is likely to be a major lithological contact within the Kidnappers Group. These markers provide supporting structural control for interpretation of SkyTEM data in this study and were imported into GeoScene3D as 2D surfer grid files. Due to depth limitations of borehole and SkyTEM data, the interpretation of layers below 500 m depth is mainly controlled by seismic data interpretations (Tschritter et al. 2022; Begg et al. 2022).

DC resistivity, GroundTEM and electrical resistivity tomography (ERT) sections (Figure 2.10; Tschritter et al. 2022) were imported into GeoScene3D as *.xyz files and provide additional resistivity information in some areas where there is no SkyTEM data coverage.

The 2018 numerical groundwater model for the Heretaunga Plains (Rakowski and Knowling 2018) was a three-layer model that used information from the 2014 Leapfrog geological model with minor modifications (Figure 2.11). The purpose of the numerical groundwater model was to provide support for defensible groundwater and surface water allocation and water-quality limit setting. The surface-confining material was numerically represented, and two layers (Layer 1 and 2) were aquifers. Layer 1 represents Holocene gravels (Q1) and Q2–4 Last Glacial gravels. Layer 2 represents deposits below the Last Glacial gravels (Q5–Q7) to a maximum depth of 250 m. The geological model unit separation utilised within this numerical model provides guidance on the hydrogeological separations of importance for numerical modelling within the Heretaunga Plains.

A piezometric contour map was developed by Rakowski and Knowling (2018) based on 289 water-level measurements covering the entire Heretaunga aquifer system, and most of the SkyTEM survey area, using data from February 1995 (Heretaunga Plains; Dravid and Brown 1997) and December 2014 (Moteo Valley, Upper Ngaruroro Valley). HBRC also undertook a smaller water-level survey in the Heretaunga Plains during January/February

2020 (Tschritter et al. 2022). These recent data show similar water levels as those of Rakowski and Knowling (2018). Additionally, they show water levels ranging from 1 to 12 m depth in the unconfined region of the aquifer, and up to 15 m depth in the upper part of the Ngaruroro River valley. As a change in saturation can provide a contrasting resistivity signal, these water levels provide an indication of depths to expect an associated signal. Water levels from these studies also provide information on the main area of flowing artesian conditions and, hence, the approximate extent of near-surface confining conditions in the survey area (Figure 2.12).

Resistivity values calculated from groundwater sample measurements in the Heretaunga Plains display a variability of 14–85 ohm.m, with lower values generally found near the boundaries of the plains and which are variable with depth (Tschritter et al. 2022). During drilling in the 1990s, sampling at research bore Awatoto showed changes from 71.9 to 25.6 ohm.m (Dravid and Brown 1997; Tschritter et al. 2022) – consistent with a measured increase in groundwater age with depth (increase in age consistent with a decrease in resistivity due to changes in total dissolved solids within the groundwater). Offshore salinity monitoring shows a resistivity value of 0.2 ohm.m, and freshwater has a resistivity value of >8.3 ohm.m (Tschritter et al. 2022). The Ahuriri Estuary is brackish or salt water throughout. The Waitangi Estuary is mostly fresh or slightly brackish, and salt water regularly extends upstream at the base of the rivers. Salt water has been reported in some bore logs at the coast near Napier within gravel in the upper 30 m (Tschritter et al. 2022).

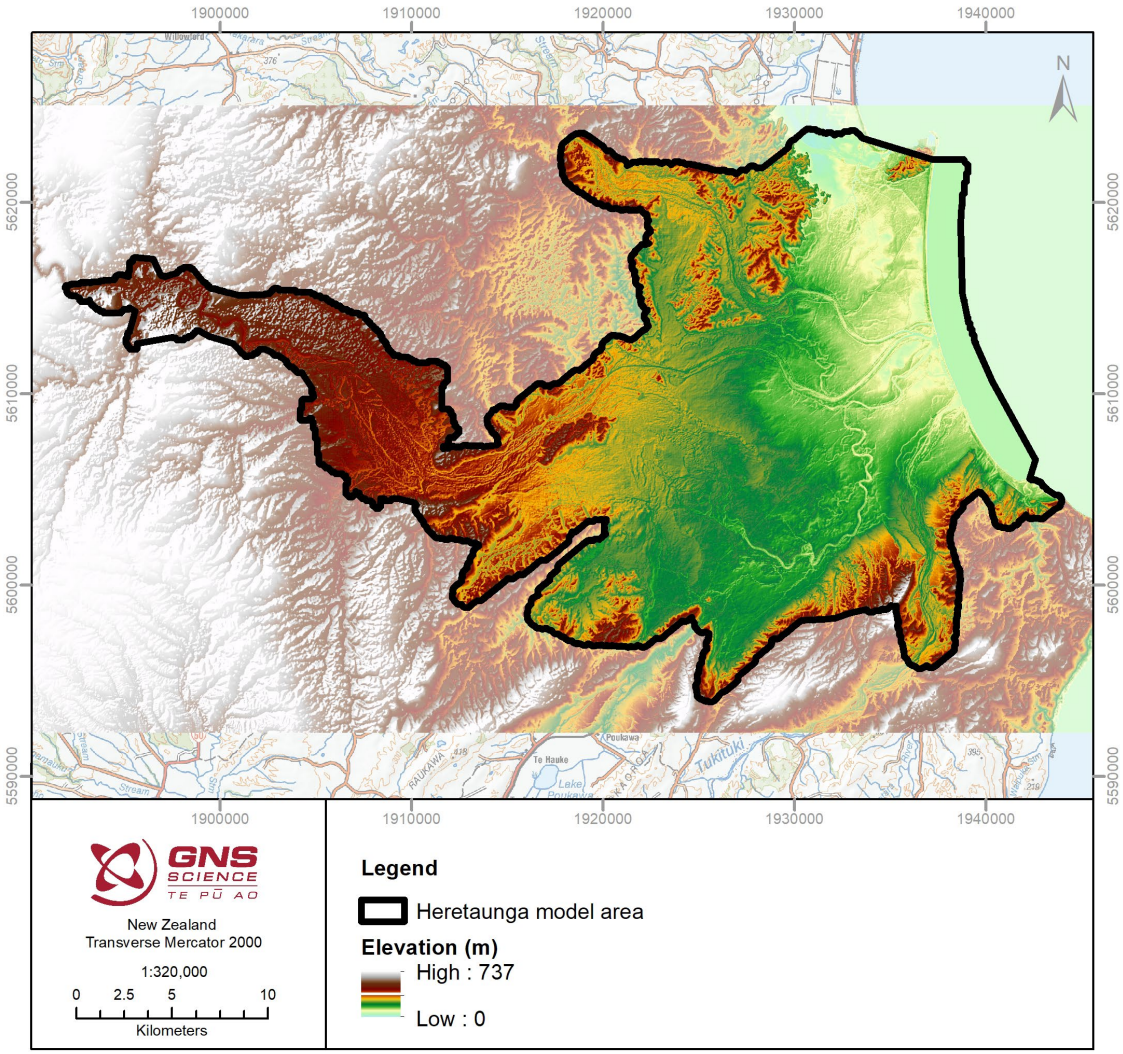


Figure 2.3 Shaded relief elevation map of the Heretaunga Plains showing the extent of the digital elevation model coverage (Farrier 2020). Figure adapted from Tschritter et al. (2022).

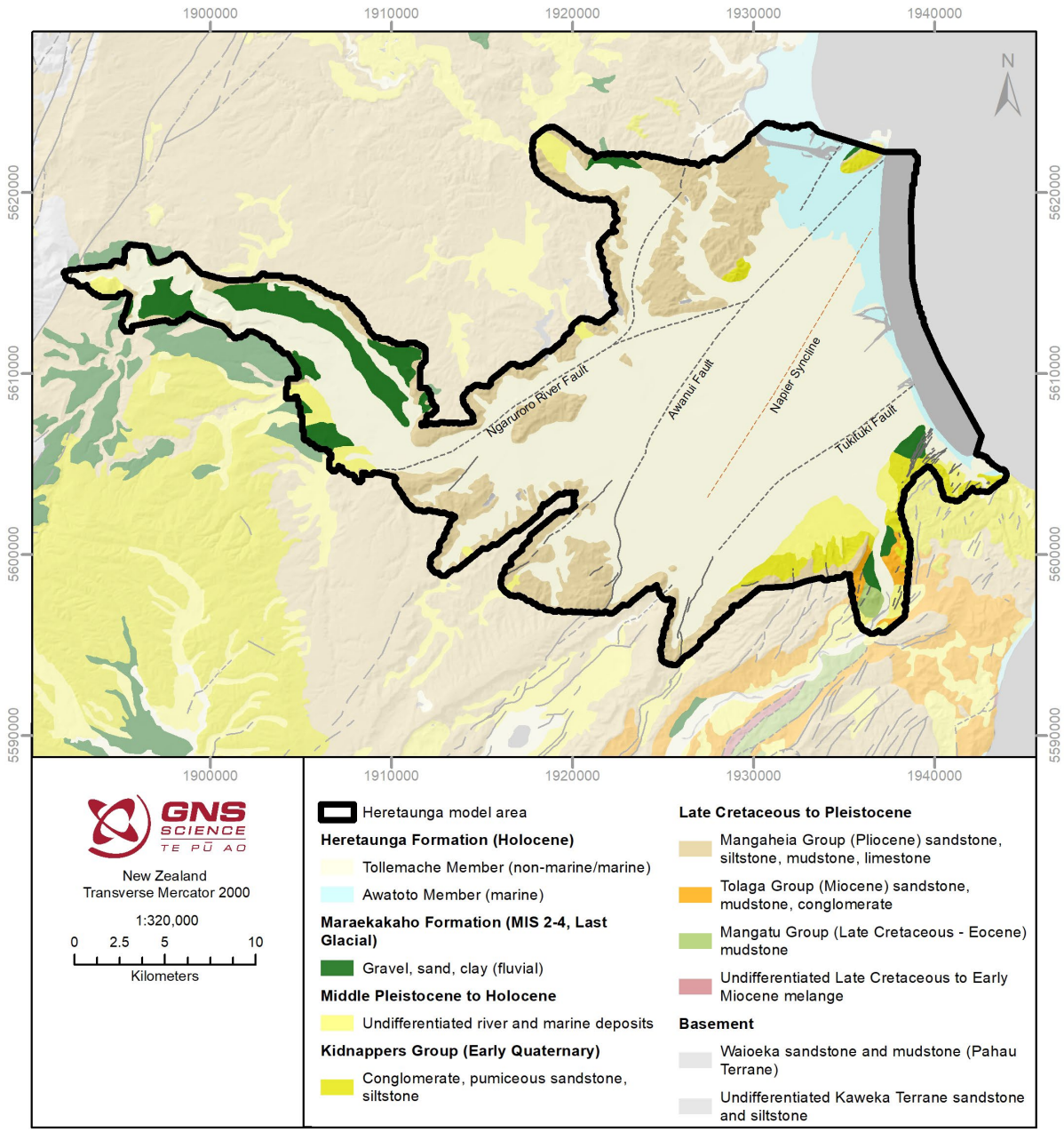


Figure 2.4 1:250,000-scale geological map of New Zealand (Heron 2020). Faults and folds in the survey area are explained in Figure 2.5. Geological units shown in the legend have been adjusted to match the recent higher-resolution urban map series naming convention shown in Figure 2.5. Figure adapted from Tschritter et al. (2022).

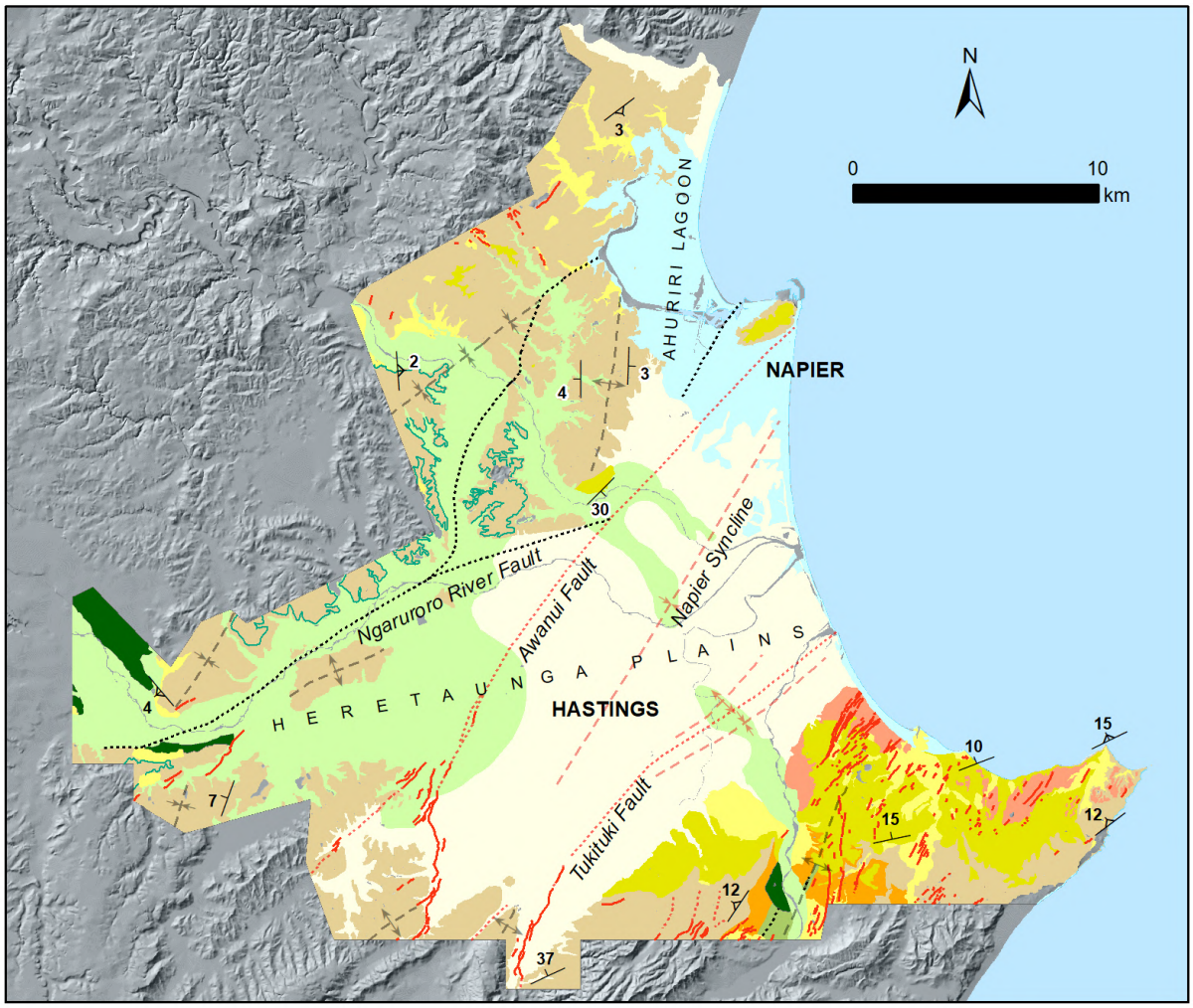


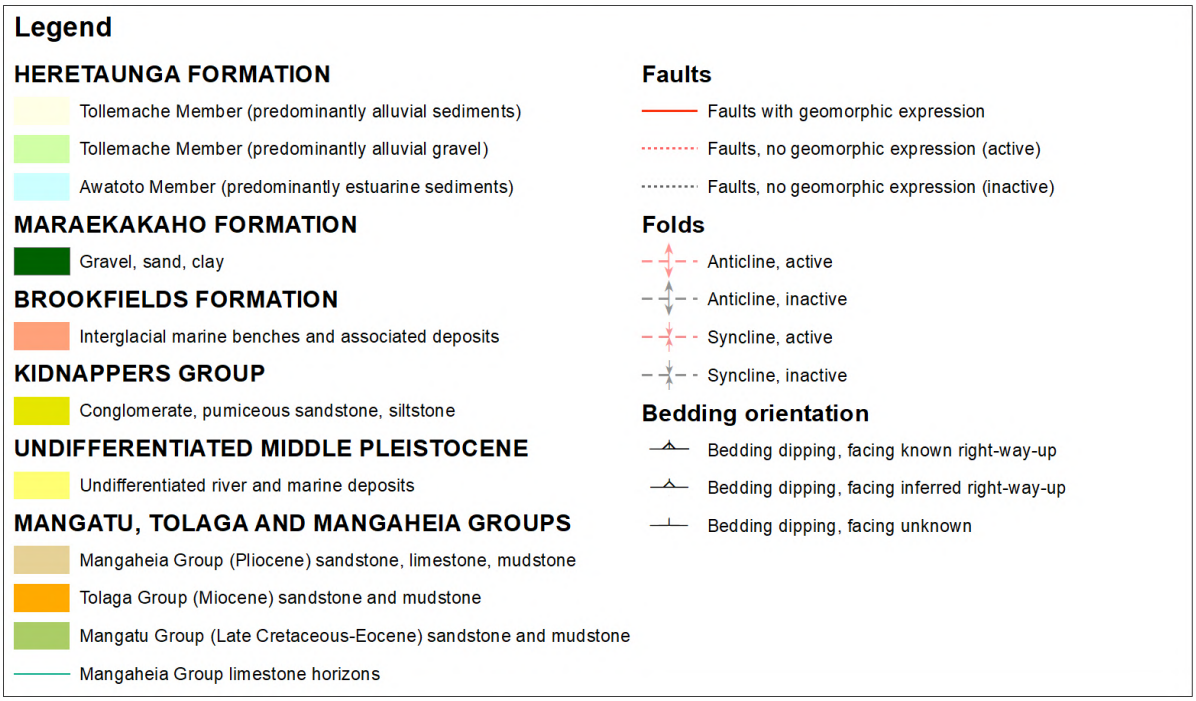


Figure 2.5 A simplified version of the 1:75,000-scale geological map of the Napier-Hastings urban areas (Lee et al. 2020). Figure from Begg et al. (2022).

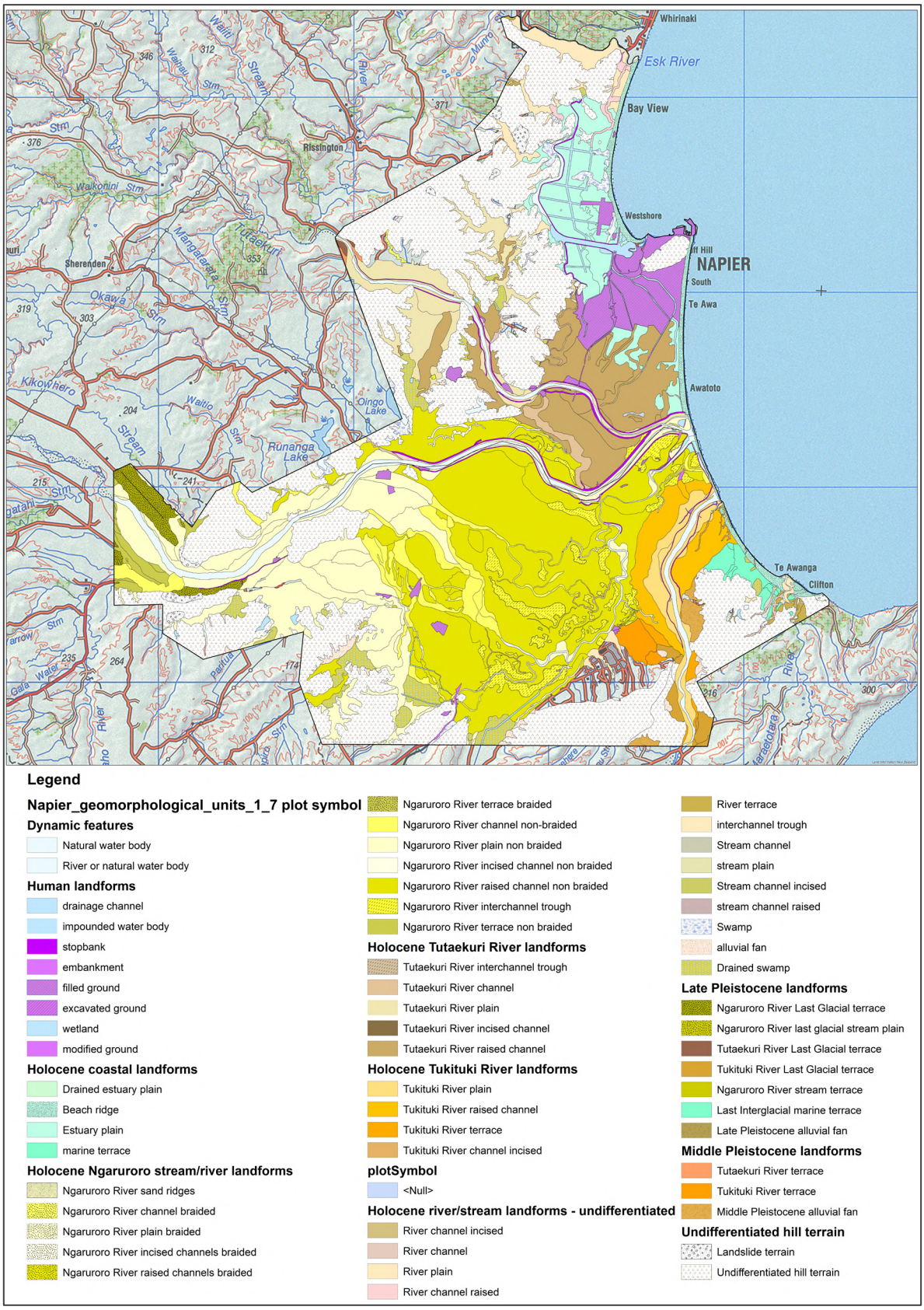


Figure 2.6 Draft geomorphological map of the Napier-Hastings urban areas at the 1:75,000 scale (Lee et al., in prep.) that maps different types of river, coastal and hill landforms in the area. Landform features associated with the Ngaruroro River are in shades of yellow, Tutaekuri River landforms are shown in brown and Tukituki River landforms in orange. The large areas of yellow show that a large part of the Heretaunga Plains is landscaped by the Ngaruroro River.

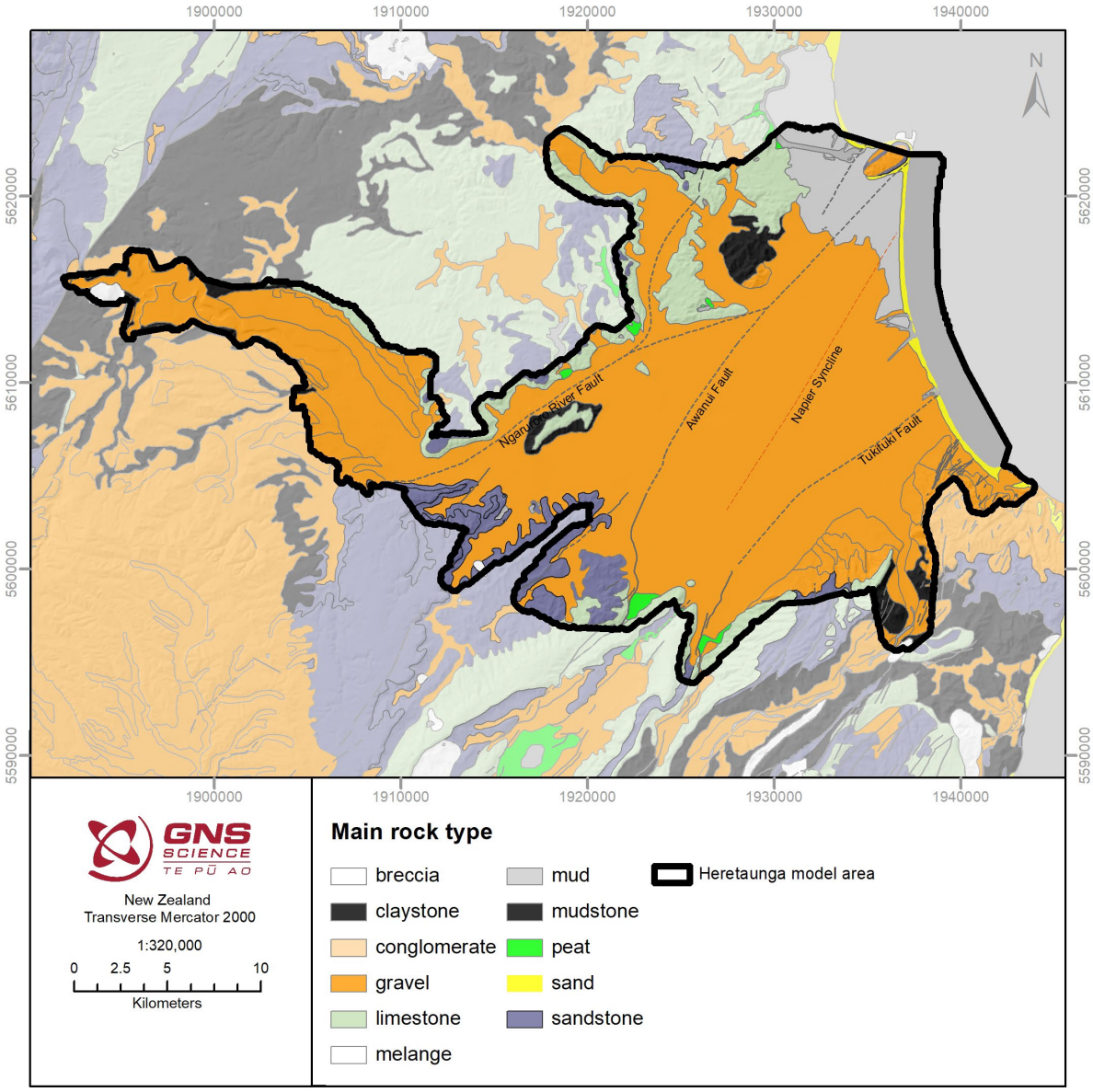


Figure 2.7 Main rock type from the 1:250,000-scale geological map of New Zealand (Heron 2020). Faults and folds in the survey area are explained in Figure 2.5.

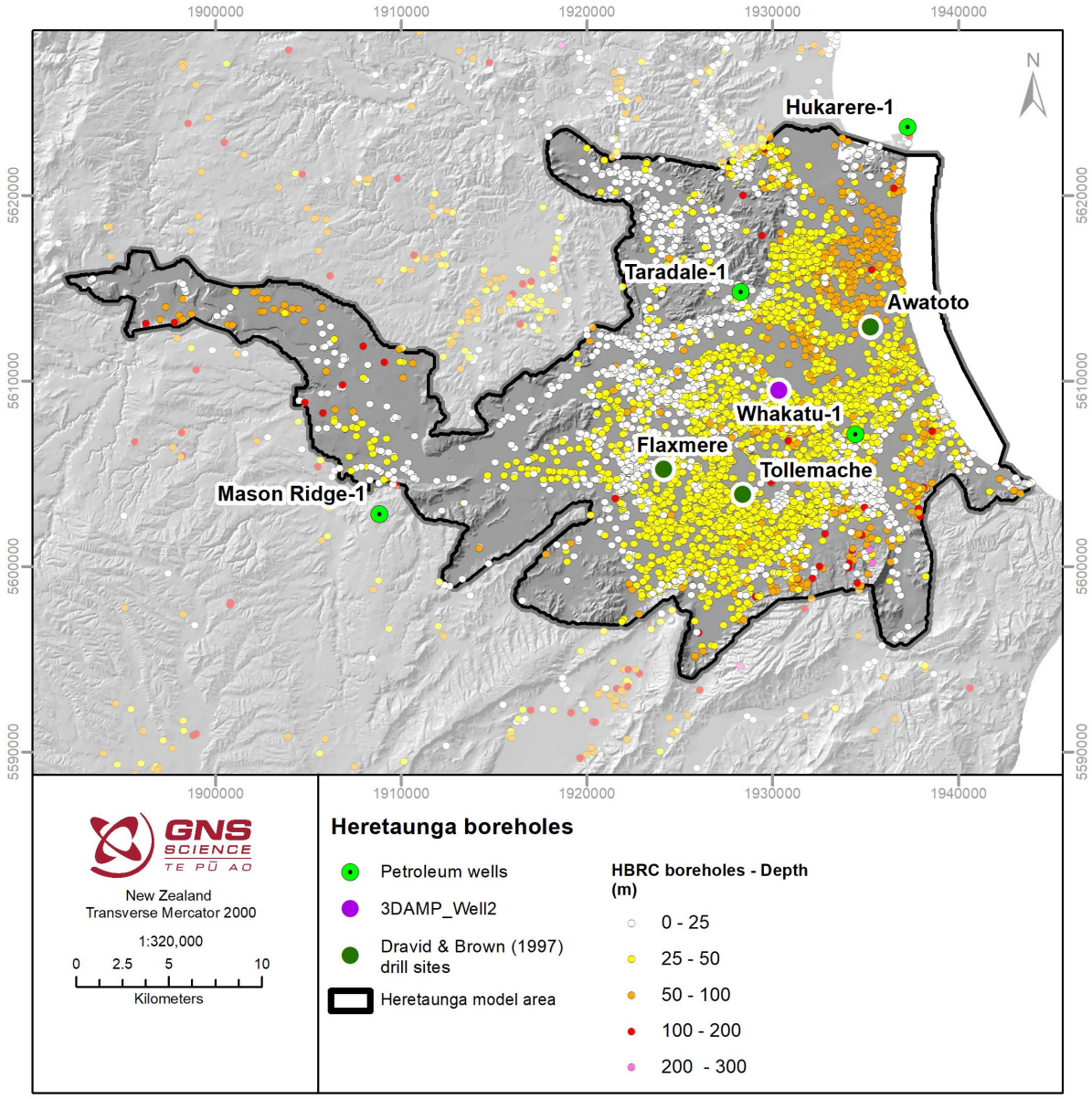


Figure 2.8 Location of available lithological logs from boreholes. HBRC boreholes are colour-coded by depth.

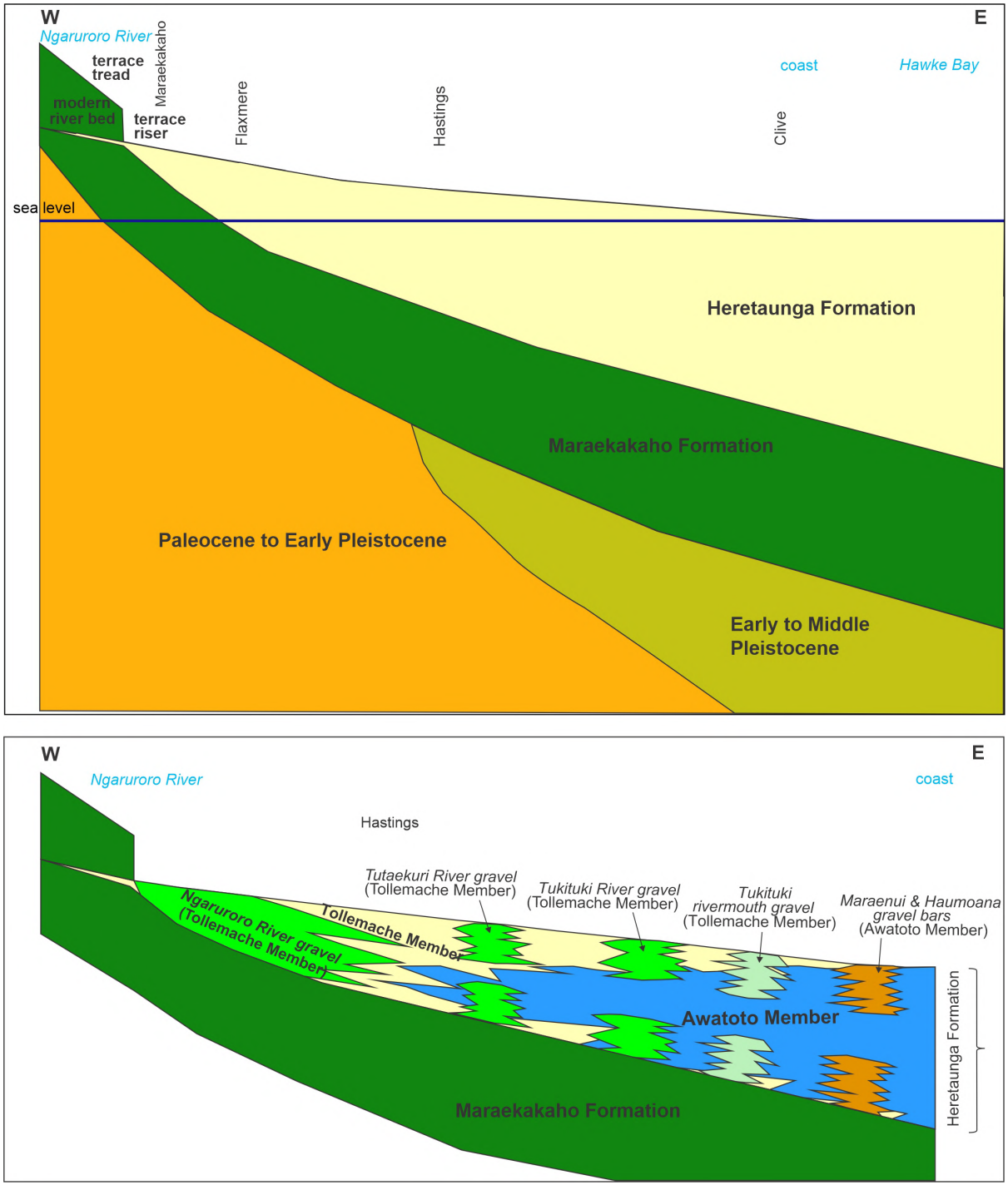


Figure 2.9 Schematic cross-sections of the conceptual stratigraphy of the subsurface geology in the Heretaunga basin from west to east highlighting (top) the major units and (bottom) sub-units within the Heretaunga Formation. Figure from Begg et al. (2022).

Table 2.2 A summary of the units defined in the subsurface geological model, with their interpreted ages and a brief description of the lithology used to define the unit. Table modified after Begg et al. (2022).

| Geological Model Unit and Lithological Descriptions | | | Age | Summary Description |
|---|---|---|---|---|
| Heretaunga Formation | Awatoto Member | Awatoto Member | Holocene (MIS 1) | Fine grained marine sand, silt and clay |
| | | Maraenui gravel bar | | Beach gravel near Napier (Lithological unit) |
| | | Haumoana gravel bar | | Beach gravel near Haumoana (Lithological unit) |
| | Tollemache Member | Tollemache Member | | Undifferentiated fine-grained non-shelly marine and non-marine sediments |
| | | Tutaekuri River gravel | | Gravel from the Tutaekuri River (Lithological unit) |
| | | Ngaruroro River gravel | | Gravel from the Ngaruroro River (Lithological unit) |
| | | Tukituki River gravel | | Gravel from the Tukituki River (Lithological unit) |
| | | Tukituki rivermouth gravel | | Gravel at the Tukituki River mouth (Lithological unit) |
| Maraekakaho Formation | Gravel, mud, silt and clay | | Late Pleistocene (Last Glacial, MIS 2–4) | Gravel from river catchments draining to the Heretaunga Basin |
| Early to Middle Pleistocene | Conglomerate, sandstone, lignite, ignimbrite, paleosols | | Early Pleistocene to earliest Late Pleistocene (MIS 5) | Rock and poorly consolidated sediment of Kidnappers Group, Brookfields Formation and other minor surficial deposits not otherwise modelled |
| Paleocene to Early Pleistocene | Sandstone, limestone, siltstone and mudstone | | Paleocene to Early Pleistocene | Rock of Mangatu Group, Tolaga Group, Mangaheia Group |

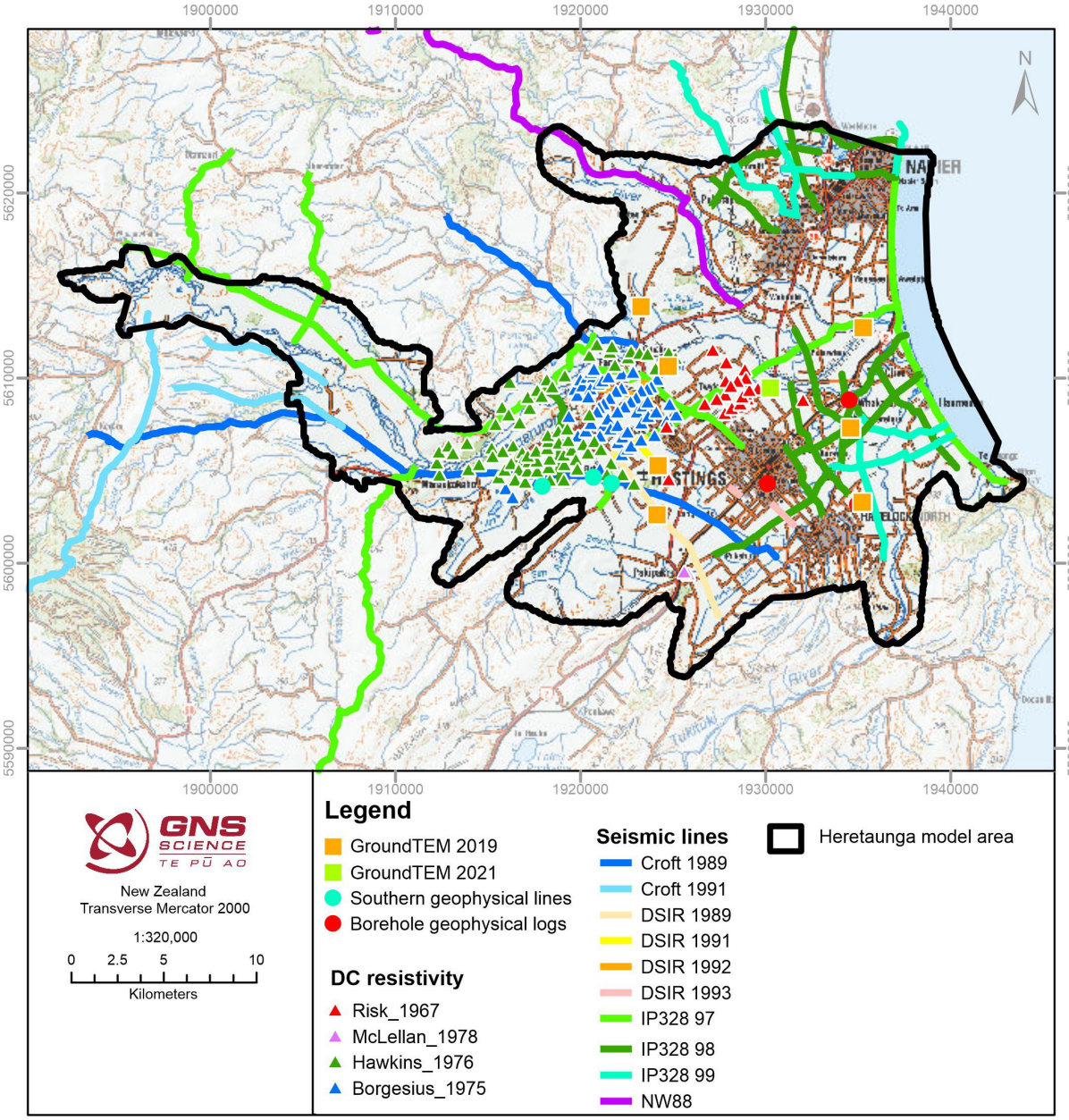


Figure 2.10 Location of seismic lines, DC resistivity soundings, groundTEM and shallow geophysical data in the Heretaunga Plains. See Tschritter et al. (2022) for details.

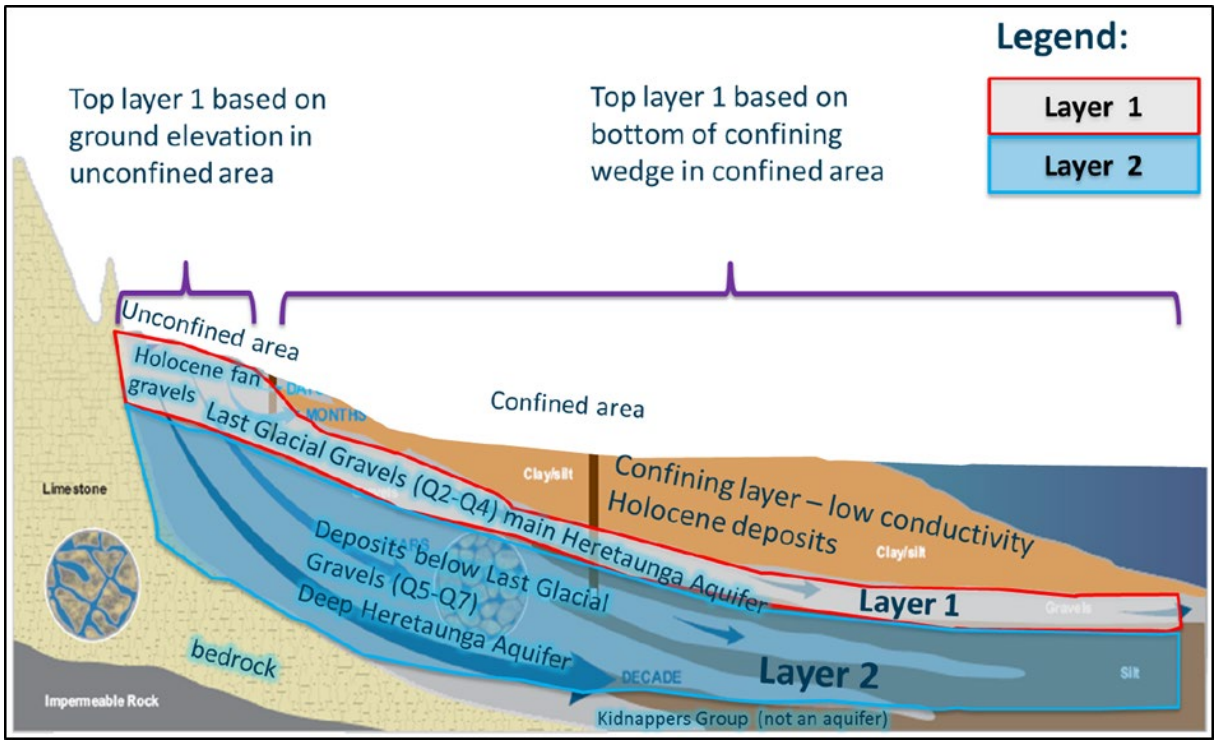


Figure 2.11 Schematic cross-section profile of the Heretaunga Plains aquifer system. Figure from Rakowski and Knowling (2018).

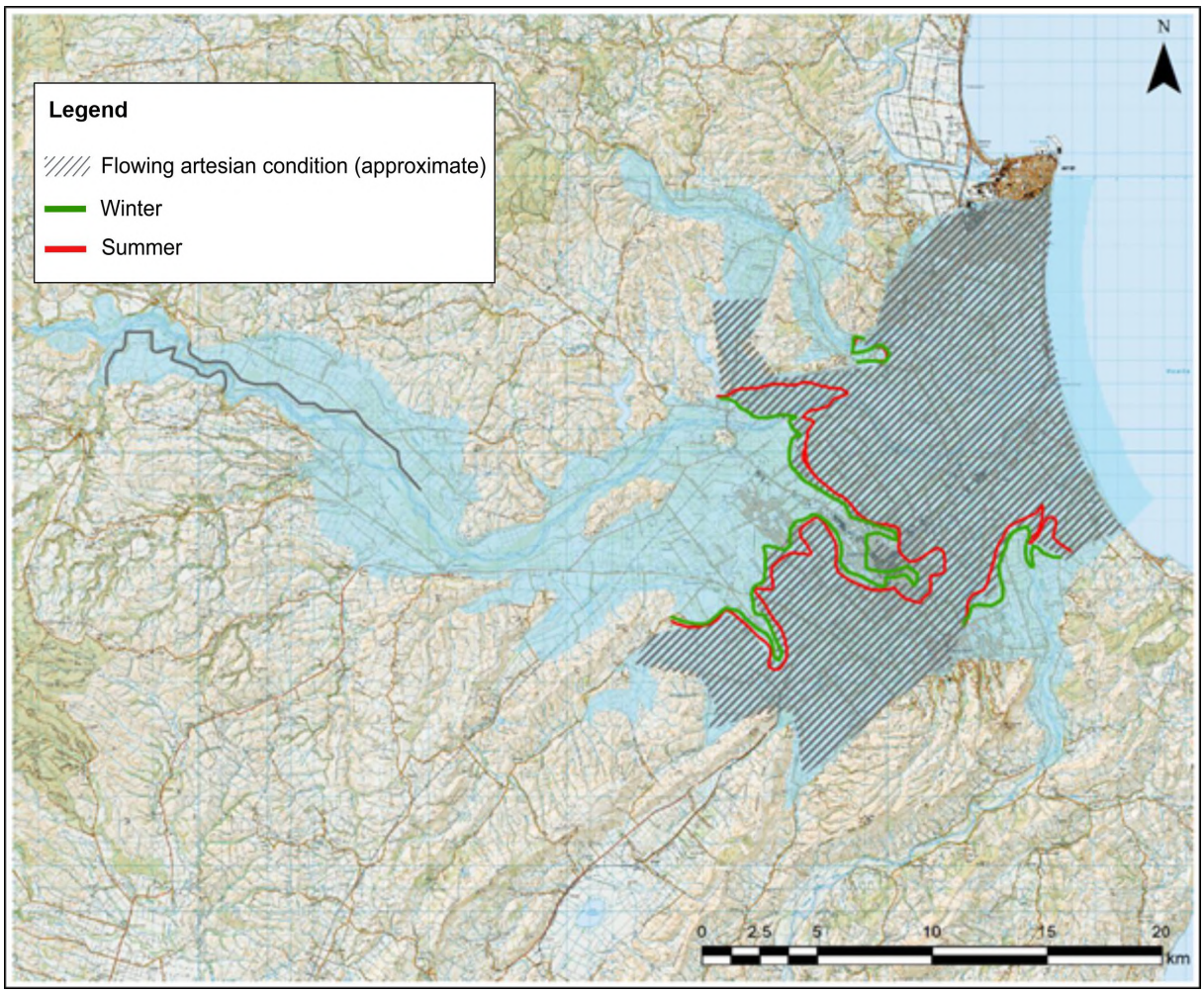


Figure 2.12 Flowing artesian conditions in the Heretaunga Aquifer. Figure adjusted from Rakowski and Knowling (2018).

## 2.3 Assessment against Deep Boreholes

Key geological markers at deep boreholes have been interpreted at different depths by various authors (Table 2.3; Dravid and Brown 1997; Paquet et al. 2009). Kellett et al. (2022) provided an assessment of information from 12 deep (>100 m) wells against resistivity models, including an interpretation of the main resistivity units, and the stratigraphic and hydrogeological implications of this interpretation. Two cross-sections through these deep wells were utilised to show six interpreted marker horizons. These marker horizons are (1) Top of marine transgression (Awatoto Member), (2) Top of gravel (MIS 1 or 2), (3) Base of gravel (Maraekakaho Formation or older), (4) Top of gravel or coarse-grained unit (Early to Middle Pleistocene), (5) Top of mudstone (Taradale/Mahanga/Makaretu Formation) and (6) Top of limestone (Scinde Island Formation).

These horizons provide information on the lateral continuity of different stratigraphic units and provide some initial guidance for mapping of the hydrogeological boundaries within this study. A summary of the resistivity units and resistivity ranges for three of the deep wells is shown in Table 2.3 (Kellett et al. 2022). Resistivity Unit 1 (RU 1) includes high-resistivity gravels of Holocene age (Tollemache Member) and the Holocene-age low-resistivity marine sediments (Awatoto Member). Resistivity Unit 2 (RU 2) is dominated by the Maraekakaho Formation gravel but also includes Holocene gravels above where there is no intervening low-resistivity layer. Resistivity Unit 3 (RU 3) consists of rock and unconsolidated sediment from Brookfields Formation, Middle Pleistocene and Kidnappers Group.

The resistivity models suggest that there may be younger and more permeable sediments at greater depths than suggested by the Dravid and Brown (1997) interpretation (Table 2.3). This resistivity model interpretation is supported by mean residence times from groundwater samples (Tschritter et al. 2022) and the Paquet et al. (2009) interpretation (Table 2.3; Kellett et al. 2022).

Table 2.3 Comparison of depth ranges of key geological times in a selection of deep boreholes interpreted by Dravid and Brown (1997), Paquet et al. (2009) and Kellett et al. (2022). Q1 is the Holocene and is equivalent to Marine Isotope Stage 1 (0–11 ka). Q2–Q4 is the last glaciation, equivalent to MIS 2 (11–24 ka), MIS 3 (24–59 ka) and MIS 4 (59–71 ka). Q5 is the interglacial interval, equivalent to MIS 5 (71–128 ka). Q6 is the Penultimate glaciation (Waimea Glaciation) and correlates with MIS 6 (128–186 ka). Q7 is the Penultimate interglacial interval (Karoro) and equates to MIS 7 (186–245 ka).

| Geological Time | Climate | Dravid and Brown (1997) Depth from / to (mbgl) | | | Paquet et al. (2009) Depth from / to (mbgl) | | Formation Name | Kellett et al. (2022) Resistivity Units (RU) |
|---|---|---|---|---|---|---|---|---|
| | | Flaxmere | Tollemache | Awatoto | Tollemache | Awatoto | | |
| Q1 | Post-glacial | 0.0–59.4 | 0.0–71.5 | 0.0–64.5 | 0.0–55.7 | 0.0–53.6 | Heretaunga Formation | RU 1<br>Awatoto Member<br>(<50 ohm.m)<br>Tollemache Member<br>(>50 ohm.m)<br>Flaxmere and Tollemache have RU 1 and RU 2 in this interval |
| Q2–Q4 | Last glaciation | 59.4–96.3 | 71.5–90.2 | 64.5–113.0 | 55.7–127.4 | 53.6–109.6 | Maraekakaho Formation | RU 2 (>100 ohm.m) |
| Q5 | Last interglacial | 96.3–137.3 | 90.2–144.0 | 113.0–117.0 | 127.4–232.8 | 109.6–221.9 | Brookfields Formation, Kidnappers Group and age-equivalent rocks | RU 3<br>(50–100 ohm.m) |
| Q6 | Penultimate glacial | - | 144.0–154.0 | 117.0–132.0 | 232.8–256.0 | 221.9–254.0 | | |
| Q7 | Penultimate interglacial | - | 154.0–256.0 | 132.0–254.0 | - | - | | |

# 3.0 METHOD

The delineation of major hydrogeological units using GeoScene3D software, includes:

- establishing a conceptual hydrogeological interpretation model, and
- manual delineation of hydrogeological units and creation of boundary grids.

## 3.1 Establishing a Hydrogeological Conceptual Interpretation Model

Using GeoScene3D software, resistivity models and supporting data (see Section 2) were visualised together in cross-section profiles and map-view slices and considered against the existing geological and hydrogeological understanding of the area (as summarised within Tschritter et al. [2022]). As expected (e.g. Figure 1.2; Rawlinson et al. 2021; Tschritter et al. 2022; Kellett et al. 2022), silt and clay/mud-dominated lithologies that form confining layers primarily have relatively low resistivity values, the gravel and sand-dominated lithologies that form the majority of the aquifers have relatively high resistivity values, and consolidated basement rocks have variable resistivity values depending on lithological composition (low resistivity values for mud-dominated and high resistivity values for limestone-dominated, e.g. Figure 2.7).

Considering subsequent hydrogeological modelling objectives, a simplified hydrogeological framework was developed that consists of the following four major hydrogeological units (HU; Table 3.1, Figure 3.1 and Figure 3.2):

- HU 1 (confining unit)
- HU 2 (shallow aquifer unit)
- HU 3 (deep aquifer unit)
- HU 4 (basement unit).

A brief description of these hydrogeological units and comparisons between this conceptual hydrogeological framework and those utilised within the recent geological and groundwater numerical models (Begg et al. 2022; Hemmings 2022; Rakowski and Knowling 2018) are provided within Figures 3.1 and 3.2 and Table 3.1. Key differences between the hydrogeological framework presented in this report and these prior models are described below:

1. Q1 deposits (Awatoto Member and Tollemache Member) are split between HU 1 and HU 2 depending on the resistivity character, areas with flowing artesian conditions and dominant lithology at different areas. This study assumes that areas containing the marine clay-silt-dominated Awatoto Member and measured flowing artesian conditions represent the lateral extent of HU 1 (confining layer). The vertical extent of HU 1 includes sediments of the Awatoto Member and overlying sediments of the Tollemache Member. Similar to the groundwater model (Rakowski and Knowling 2018), the remaining terrestrial sediments of Q1 (lithologies ranging from clay to gravel of the Tollemache Member) are grouped under HU 2 (shallow aquifer).
2. Q5 (Dravid and Brown [1997] interpretation) is split between HU 2 and HU 3 because Q5 displays a variable resistivity character. The uppermost high-resistivity unit of Q5 of Dravid and Brown (1997) at Flaxmere and Tollemache wells has been included as part of HU 2 and the lower-resistivity unit is included as part of HU 3. This interpretation is supported by the Paquet et al. (2009) stratigraphic interpretations at Tollemache (Table 2.3), which would place all of Q5 in our HU 3, and the assessment of Kellett et al. (2022).

3. Kidnappers Group is included within HU 3 rather than HU 4 (consistent with the 2022 geological model but not the numerical models, which were based on the 2014 geological model[1]) because some of the intervals within Kidnappers Group show high resistivity in the SkyTEM data and sand/gravel-rich sediments in the Whakatu-1 petroleum well.

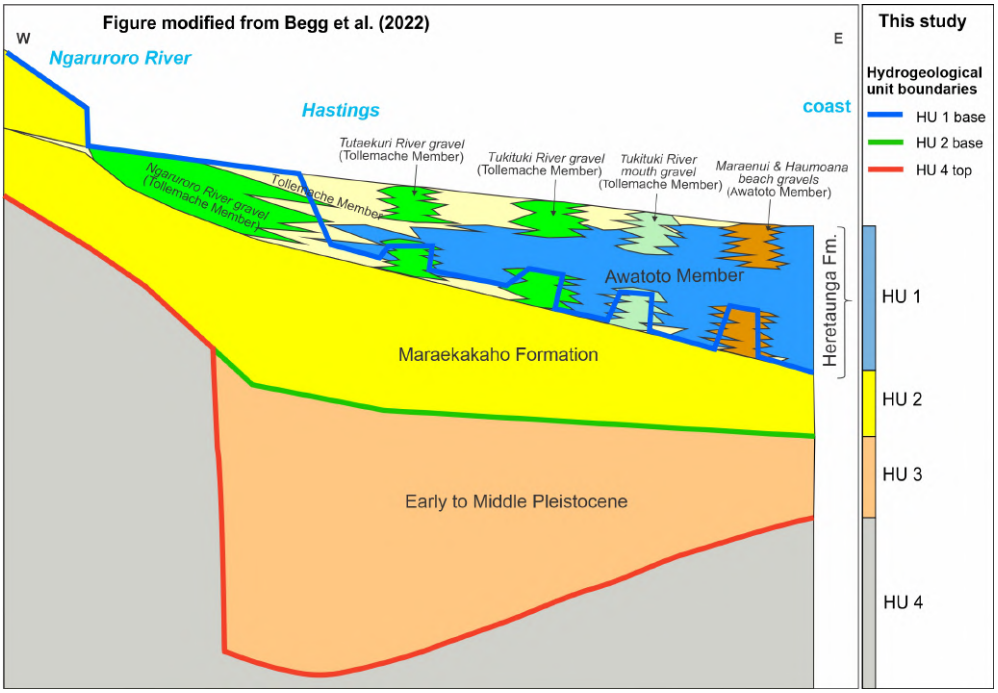


Figure 3.1 Schematic cross-section of the conceptual stratigraphy of the subsurface geology in the Heretaunga Plains from west to east. Figured modified from Begg et al. (2022). Major hydrogeological units in this study are shown in the right-hand panel for comparison to the 2022 geological model (Begg et al. 2022). Interpretations of the hydrogeological unit boundaries in this study (blue, green and red lines) are also shown on the cross-section profile.

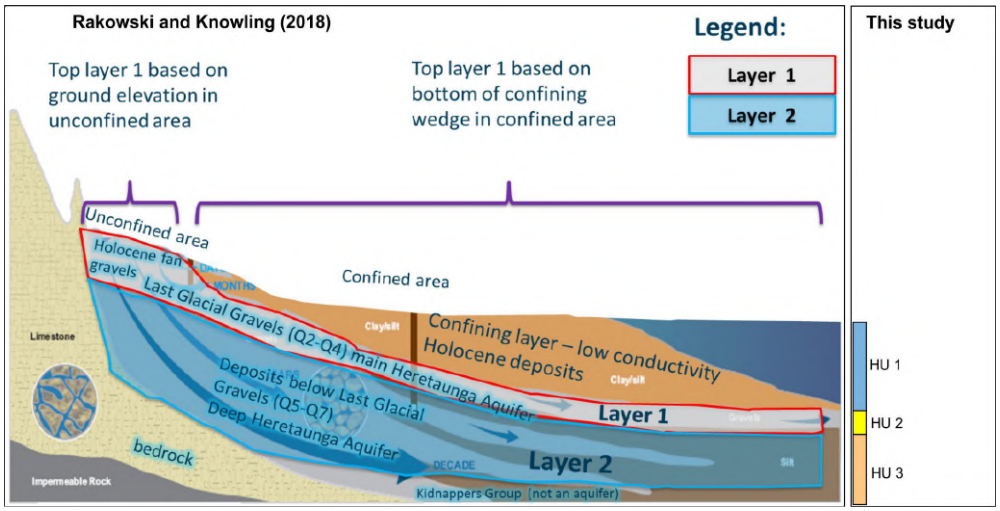


Figure 3.2 Schematic cross-section profile of the Heretaunga Plains aquifer system. Figure modified from Rakowski and Knowling (2018). Major hydrogeological units in this study are shown in the right-hand panel for comparison with the previous numerical groundwater model. HU 4 is not depicted but is equivalent to the bedrock and impermeable rock depicted on the left-hand side of the schematic.

1 The numerical groundwater models defined hydrogeological basement as the top of Kidnappers Group or at 250 m depth (where the top of Kidnappers Group extended deeper than 250 m), utilising the 2014 geological model. This top of Kidnappers Group surface within the 2014 geological model was based on conceptual depositional process assumptions rather than data. The high uncertainty in this surface was partially why it was removed in the 2022 geological model development.

Table 3.1 Brief description of the major hydrogeological units (HU) used in this work and comparison to the previous geological and numerical groundwater models. Schematic displays are also shown in Figure 3.1 and Figure 3.2.

| Name | Resistivity Character | Hydrogeological Character | Geological Equivalence (after Kellett et al. [2022]) | Geological Model 2022 Equivalence (Begg et al. 2022) | Numerical Model 2018 Equivalence (Rakowski and Knowling 2018) | Numerical Model 2022 Equivalence (Hemmings 2022) |
|---|---|---|---|---|---|---|
| HU 1<br>(confining unit) | Low to moderate resistivity | Uppermost confining layer | Holocene (Q1) deposits; includes clay-silt-dominated lithology of the Awatoto Member and the overlying lithologies of the Tollemache Member | Awatoto Member of the Heretaunga Formation model unit, including the Maraenui and Haumoana gravel bar model units. Also includes some of the riverbed and rivermouth gravels (Tutaekuri, Ngaruroro and Tukituki rivers) of the Heretaunga Formation that overlie the Awatoto Member model units | Numerically represented confining layer | Layer 1 and Layer 2 |
| HU 2<br>(shallow aquifer unit) | High resistivity across the majority of the study area. However, shows low to moderate resistivity in areas close to the hills and in some inner parts of the rivers (mostly clay-silt, with minor sand-gravel units of Tollemache Member) | Aquifer | Q1–Q4 deposits; includes Maraekakaho Formation and all terrestrial sediments of the Heretaunga Formation (Tollemache Member) that do not overlie the clay-silt-dominated sediments of the Awatoto Member | Includes sediments of the Maraekakaho Formation model unit and some of the riverbed and rivermouth gravels (Tutaekuri, Ngaruroro and Tukituki rivers) of the Heretaunga Formation that do not overlie the sediments of Awatoto Member, as well as the uppermost portion of the Early to Middle Pleistocene model unit | Layer 1 | Layers 1, 2, 3, 4, 5 |
| HU 3<br>(deep aquifer unit) | Alternating layers of low and high resistivity | Secondary aquifer | Early to Middle Pleistocene deposits; includes Q5–Q7 deposits (Brookfields Formation) and Kidnappers Group | Early to Middle Pleistocene model unit | Layer 2 (excluding Kidnappers Group) | Layers 6, 7, 8<br>(excluding Kidnappers Group) |
| HU 4 (basement unit) | Low resistivity, with some high resistivity in limestone areas | Hydrogeological basement, discrete water resources within limestone areas | Paleocene–Pleistocene consolidated rocks. | Paleocene to Early Pleistocene model unit | Hydrogeological basement (including Kidnappers Group) – no flow boundary | Hydrogeological basement (including Kidnappers Group) – no flow boundary set when basal; flux enabled when lateral |

This page left intentionally blank.

## 3.2 Manual Delineation of Hydrogeological Boundaries and Creation of Boundary Grids

Using GeoScene3D software, resistivity models and supporting data (see Section 2) were visualised together in cross-section profiles along flight lines. A maximum distance of 200 m was applied for the projection of boreholes onto the cross-sections. Resistivity models were displayed with a range of 0–200 ohm.m to highlight the resistivity contrasts identified on preliminary inspections of the data.

The smooth resistivity model was primarily used for boundary mapping, as it provides finer-detailed discrimination of sediments compared to the sharp resistivity model. The sharp resistivity model was used as a supporting reference and to assist with mapping hydrogeological boundaries with reduced uncertainty, particularly in areas of increased ambiguity and thin sediments. Resistivity contrasts were analysed, along with the borehole lithology, surface geology and mapped faults, to understand their relationship with any hydrogeological boundaries.

The top of the hydrogeological model is provided by a 25 m DEM (Section 2.2.2). In structurally complex areas (e.g. close to faults), and in areas where resistivity data have a shallow DOI or were missing, surface geology, borehole lithology and DEM data provided regional geological and structural information to enable boundary delineation. In general, the uncertainty in boundary interpretation is higher in structurally complex areas (close to faults) and close to the hills. Uncertainty also increases with distance from seed points (manually placed interpretation points) due to boundary interpolation uncertainties.

Three boundaries were manually delineated to create the four hydrogeological units (Table 3.2):

1. HU 1 base
2. HU 2 base
3. HU 4 top.

GeoScene3D software was used to interpret the hydrogeological unit boundaries as follows:

- A minimum bed thickness of ~5 m was taken as a mappable hydrogeological unit.
- Seed points (manually placed interpretation points) were interpreted at ~100 m intervals in the cross-sections where sharp resistivity contrasts were observed (Figure 3.3).
- Seed points were gridded using a kriging algorithm (ordinary kriging, octant search = 6, search ellipsis = 2000 m, node spacing = 50 m) to prepare 3D boundaries (hydrogeological unit boundaries; Figure 3.4).
- The 3D boundaries were reviewed, and additional seed points were added where needed to ensure boundary consistency with information such as structural geology, surface geology and borehole lithology (particularly in areas with gaps in the resistivity data or shallow DOIs).
- The three gridded surfaces defining the hydrogeological boundaries (HU 1 base, HU 2 base and HU 4 top) were exported from Geoscene3D, re-sampled to 25 m grids and extended over the entire survey area. Following a stratigraphic order with HU 4 top as the oldest and HU 1 base as the youngest subsurface boundary, younger units were assigned to onlap onto the older units. To enable hydrogeological unit thickness estimates, additional extended surfaces were created that were assigned the DEM elevation at locations where the hydrogeological boundaries were above the ground surface.

- The three gridded surfaces were refined at the ground surface using supplementary information:
  - Polygons of the basement, Early Pleistocene to Q5 and sediments overlying basement (Figure 3.5) were utilised to clearly demarcate the surface geological boundaries of HU 2, HU 3 and HU 4. To create these polygons, the 1:75,000-scale geological map (Lee et al. 2020) was utilised where available, and any gaps in the Heretaunga model area were filled using the 1:250,000-scale geological map (Heron 2020).
  - A Heretaunga flowing artesian area polygon was created and utilised to demarcate the HU 1 surface geological boundary (Figure 3.5). This polygon was derived from an integrated analysis of the area showing flowing artesian conditions (Figure 2.12) from Rakowski and Knowling (2018), bore locations with flowing artesian conditions and the average SkyTEM-derived resistivity of the upper 15 m (Figure 3.6). Areas falling within this boundary were considered part of HU 1. Areas outside this boundary were considered part of HU 2.

Table 3.2 Hydrogeological unit boundary delineation.

| Name | Primary Target | Additional Comments |
|---|---|---|
| HU 1 base | Base of first low-resistivity confining unit (Figure 3.3). | The area showing flowing artesian conditions was used to further edit the HU 1 base layer. Areas falling within this boundary were considered part of HU 1. Areas outside this boundary were considered part of HU 2. |
| HU 2 base | Base of high-resistivity unit occurring below HU 1 base (top of Q5–Q7 confining unit and Early–Middle Pleistocene units; Figure 3.3). | - |
| HU 4 top | Base of the lowermost moderate- to high-resistivity unit (Figure 3.3). | In some areas (mainly in the central region), HU 4 top occurs below the extent of the resistivity models. As such, seismic data (Tschritter et al. 2022) and previous geological model boundaries (Begg et al. 2022) were utilised to map the hydrogeological basement through this area (Figure 3.3). |

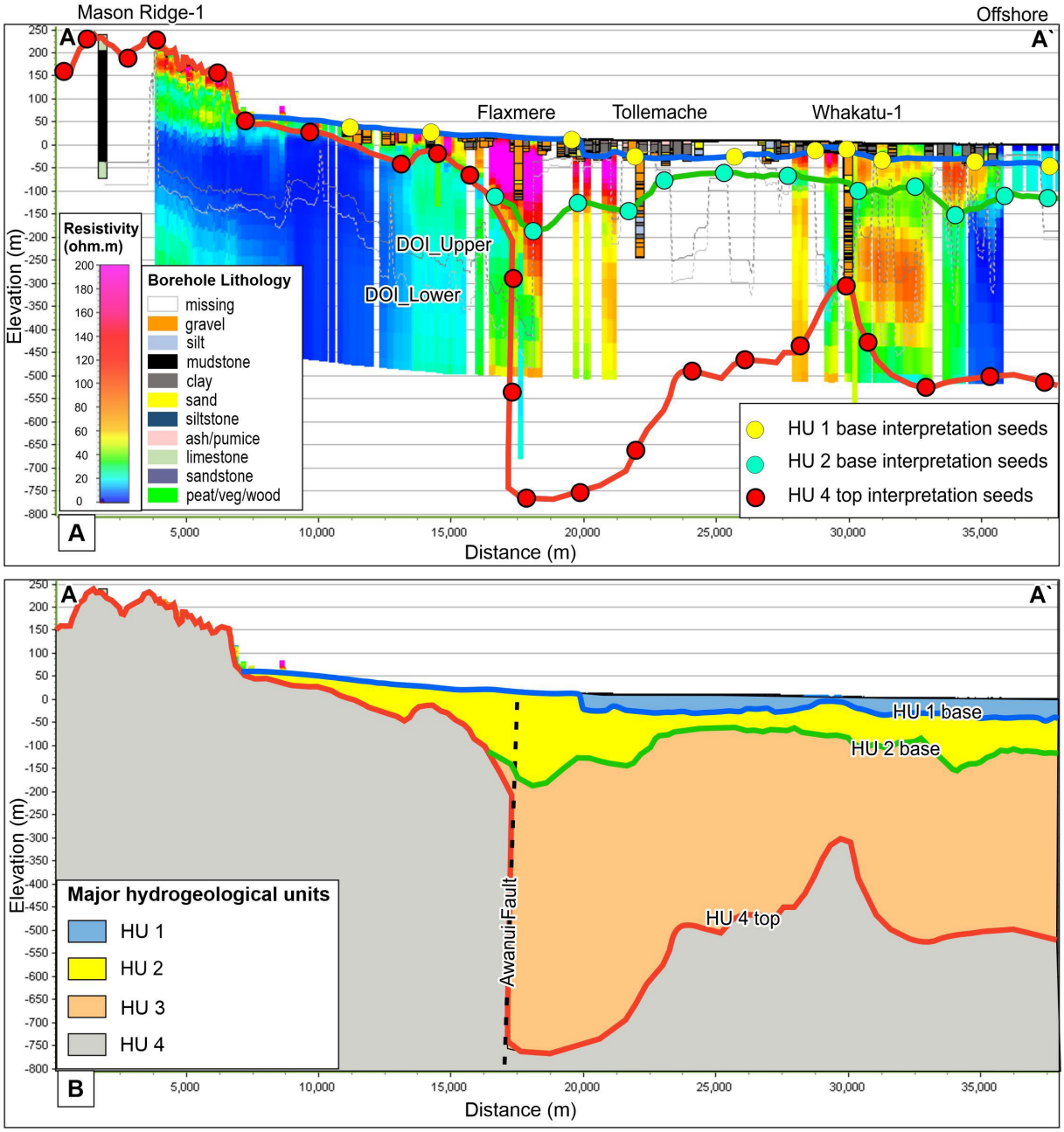


Figure 3.3 (A) West–east resistivity profile (A–A`; see location in Figure 2.1) across the study area showing the conceptual interpretation seeds and resultant boundaries for each hydrogeological unit (HU). DOI_Lower and DOI_Upper are shown as grey dashed lines on the resistivity data. Borehole data and surface geology provide calibration for the HU interpretation. (B) 2D profile of the major hydrogeological units, delineated utilising the HU boundaries from (A).

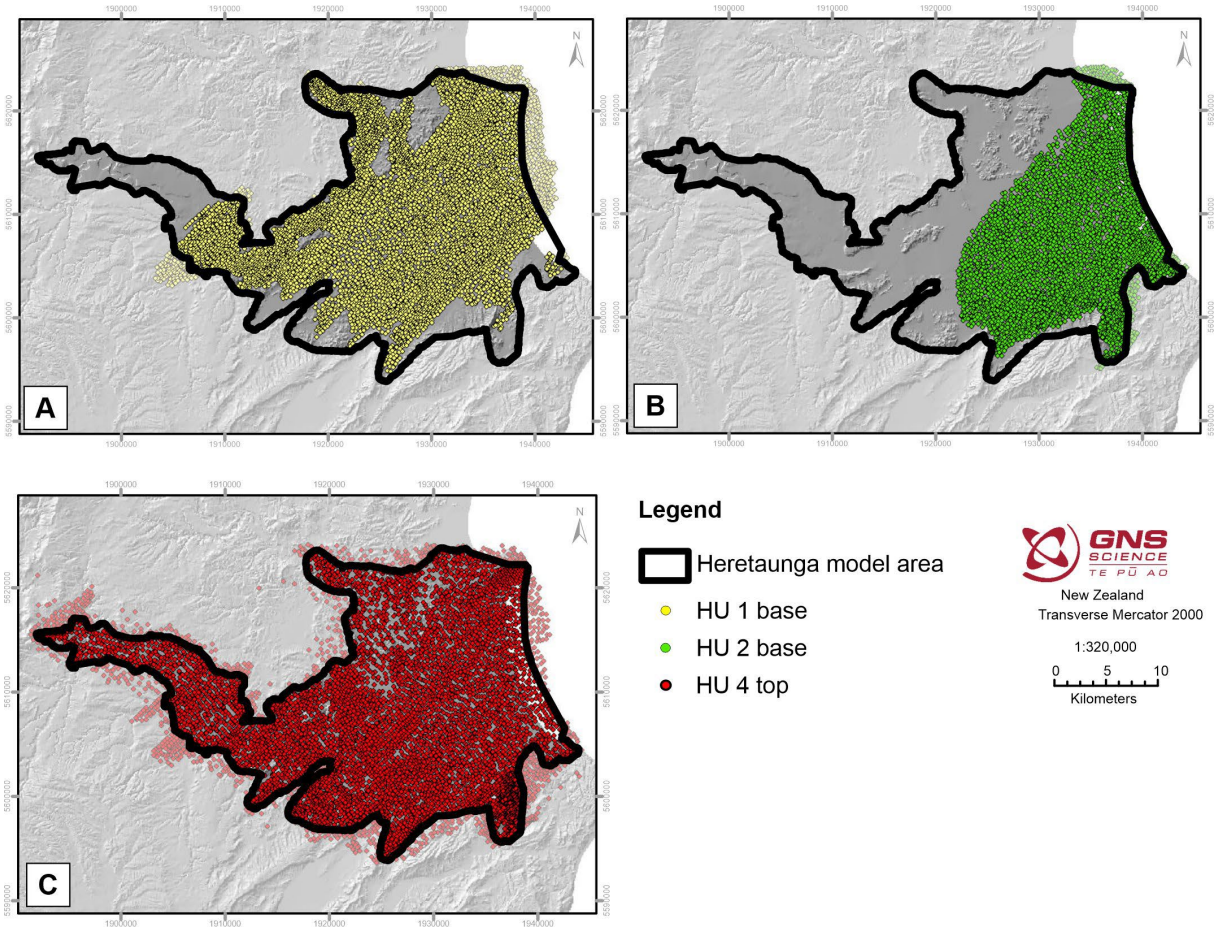


Figure 3.4 Distribution of interpretation seed points for (A) HU 1 base, (B) HU 2 base and (C) HU 4 top.

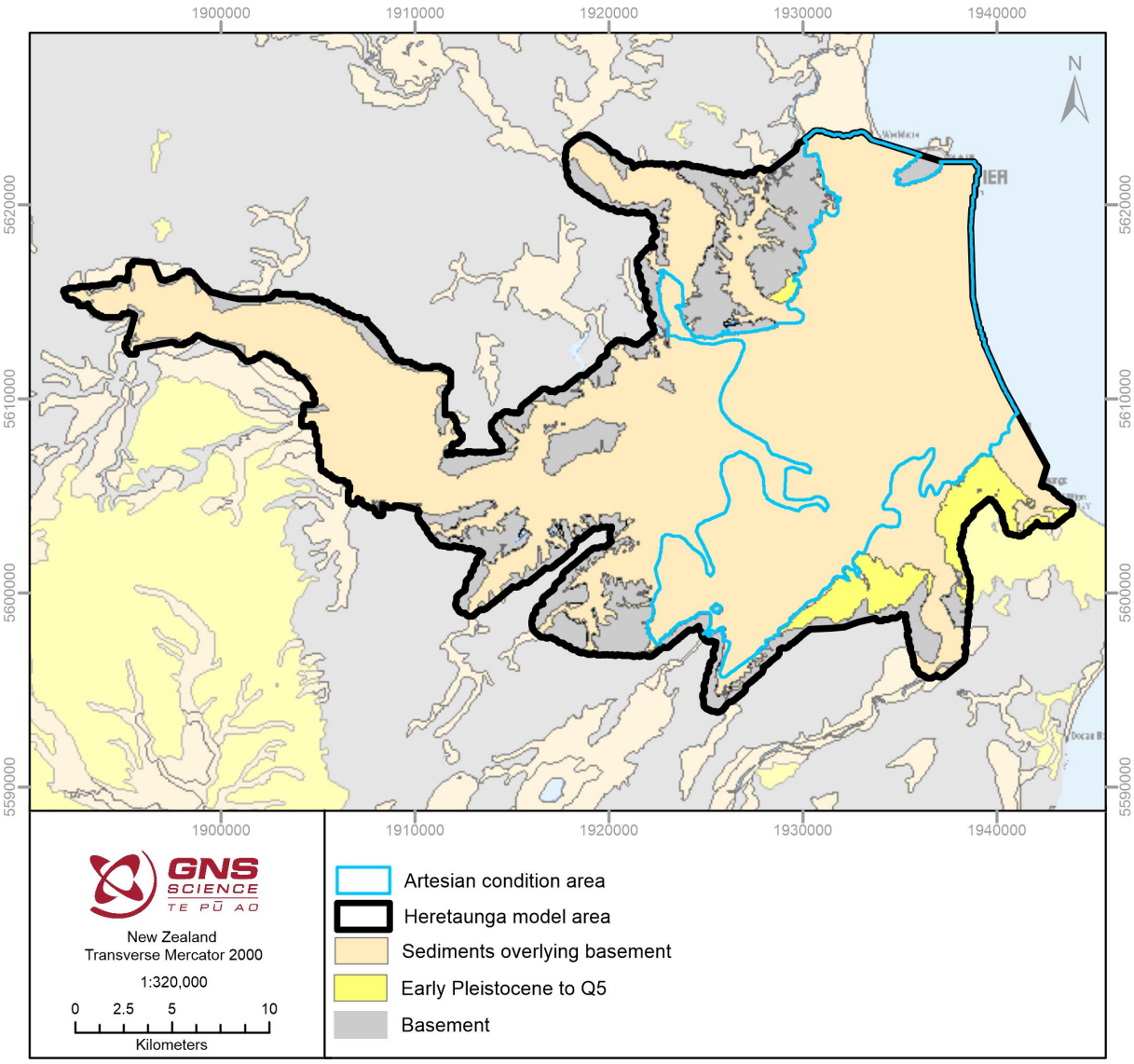


Figure 3.5 Polygons that were used to refine the hydrogeological boundary grids. These polygons show areas of basement, sediments overlying basement, Early Pleistocene to Q5 and flowing artesian condition within the Heretaunga model area.

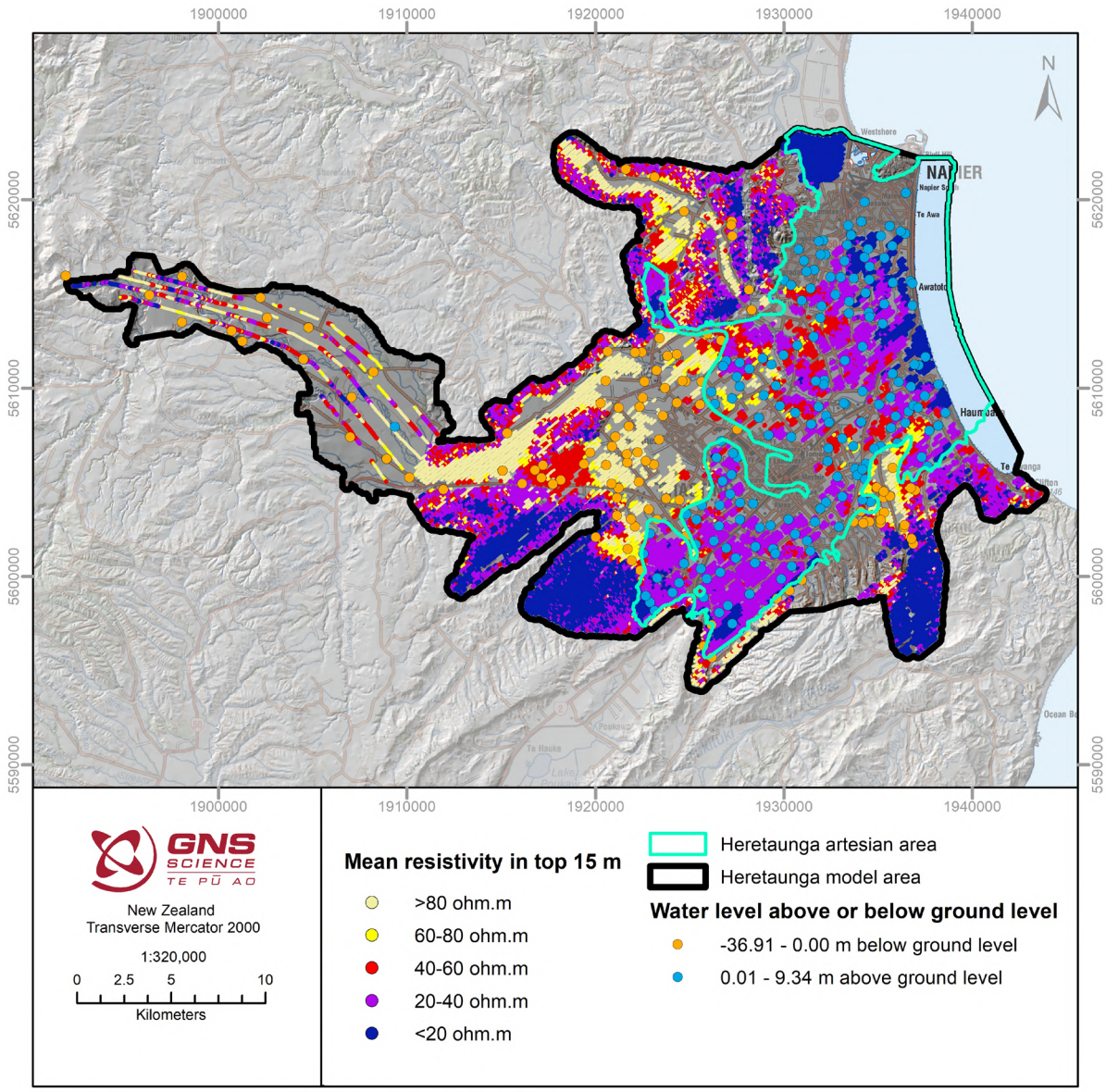


Figure 3.6 Mean resistivity map of the upper 15 m of the SkyTEM-derived sharp resistivity model. Water levels above or below ground level and the Heretaunga flowing artesian area polygon are also displayed.

# 4.0 RESULTS

Using the SkyTEM-derived resistivity models and supporting information, a simple four-layer hydrogeological model was created for the Heretaunga model area that consists of:

- HU 1 (confining unit)
- HU 2 (shallow aquifer unit)
- HU 3 (deep aquifer unit)
- HU 4 (basement unit).

This four-layer model was defined by the DEM and the manually delineated boundaries:

1. HU 1 base
2. HU 2 base
3. HU 4 top.

Comparisons to previous models and geological interpretations are provided in Section 3.1.

## 4.1 HU 1 (Confining Unit)

HU 1 represents the uppermost confining unit of this simple four-layer model of the aquifer system (Figure 4.1). The lateral extent of this confining unit was limited by a Heretaunga flowing artesian area polygon, which was developed using information on flowing artesian conditions and the average resistivity values of the upper 15 m (see Section 3.2). The top of HU 1 is defined by the DEM, and the HU 1 base boundary is defined by the base of the uppermost low-resistivity group (mainly <40 ohm.m).

HU 1 predominantly shows a low resistivity (~0–40 ohm.m); however, in some places in the central, eastern and coastal regions, it contains some thin moderate- to high-resistivity (up to ~120 ohm.m) material overlying the low-resistivity material (e.g. Figure 4.1). As the moderate- to high-resistivity material is thin and interfingers with the low-resistivity material, it is difficult to separate these two groups across the entire region. Hence, we have grouped them together as HU 1. Borehole data and previous studies in this area (e.g. Dravid and Brown 1997) suggest that the low-resistivity areas are composed of mainly silt-clay lithologies with minor sand/gravel Q1 deposits (Figures 4.1–4.2). The overlying moderate- to high-resistivity areas are mainly composed of sand/gravel-dominated lithology of the present-day (Q1) gravel fan and riverbed deposits. Where this layer is mainly clay, it shows resistivity <20 ohm.m. With increasing percentages of silt, sand and sometimes gravel lenses, it shows higher resistivity. A sharp change in resistivity at the base of this layer is observed where the gravel beds underlie the clay-rich lithologies (Figures 4.1–4.2). In areas where there is no or limited resistivity data, or where a resistivity contrast is not very clear in the cross-sections, the borehole data and surface geological map provide lithological information to map the base of this layer.

HU 1 extends over the eastern and central part of the study area (Figure 4.3). Sediment thickness of this layer increases towards the near-shore regions to a maximum thickness of 64 m (Figure 4.3). Borehole data in the area suggest that it is dominated by marine and marginal marine deposits with some minor present-day river/fan and estuary deposits. The thickness of this layer indicates that marine transgression and the main sedimentation occurred along a NE–SW trend (Figure 4.3) during the Holocene.

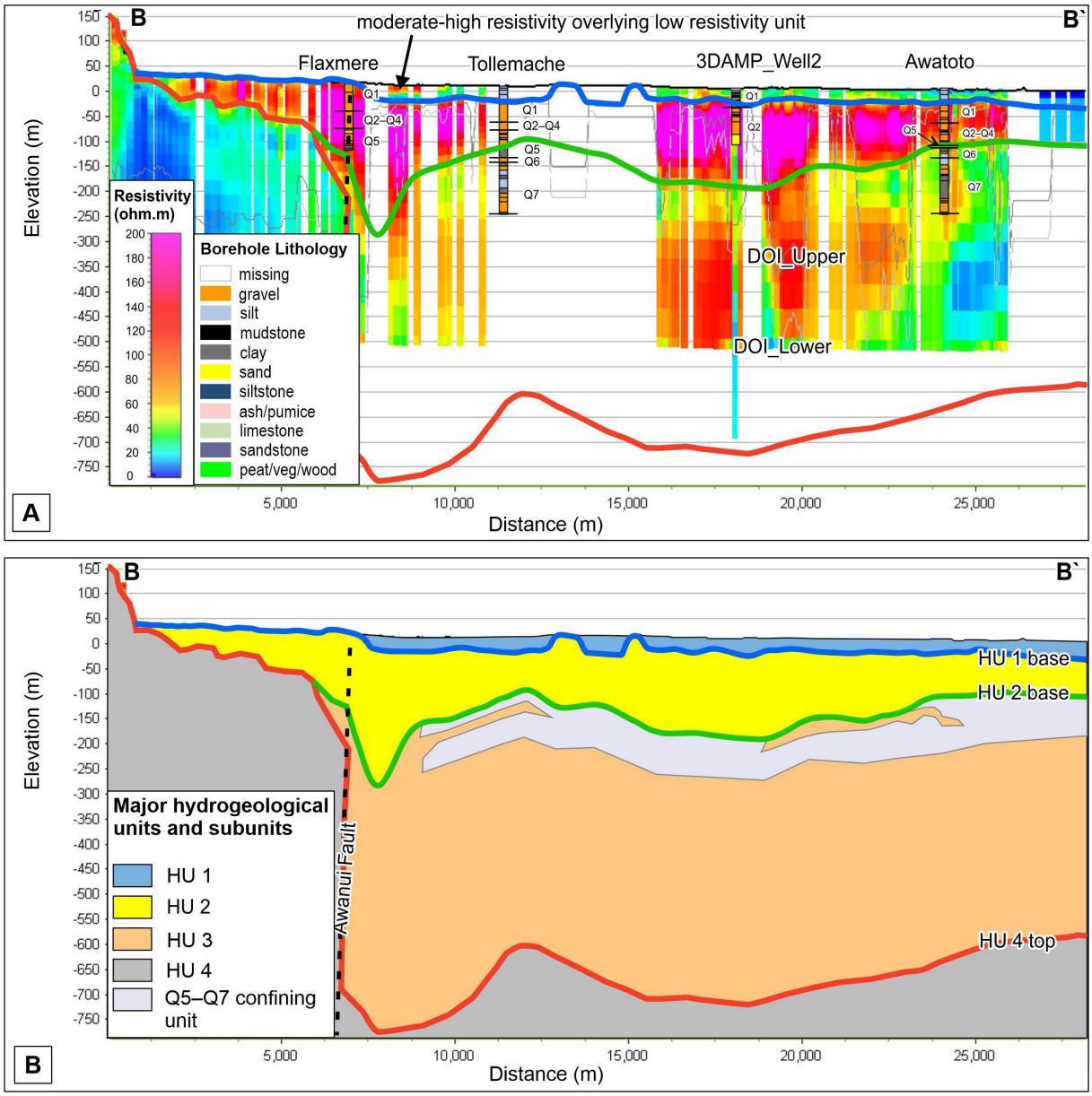


Figure 4.1 (A) West–east resistivity profile (B–B`; see location in Figure 2.1) across the study area showing the boundaries for each hydrogeological unit (HU). DOI_Lower and DOI_Upper are shown as grey dashed lines on the resistivity data. (B) Hydrogeological interpretation based on the boundaries delineated in (A). The Q1–Q7 markers shown at wells are from David and Brown (1997) to indicate the approximate age range of the interpreted hydrogeological units. Note: the interpretation of a Q5–Q7 confining unit in Figure 4.1b is mainly conceptual; it is displayed as it assisted with the HU 2 base boundary delineation (see Table 3.2).

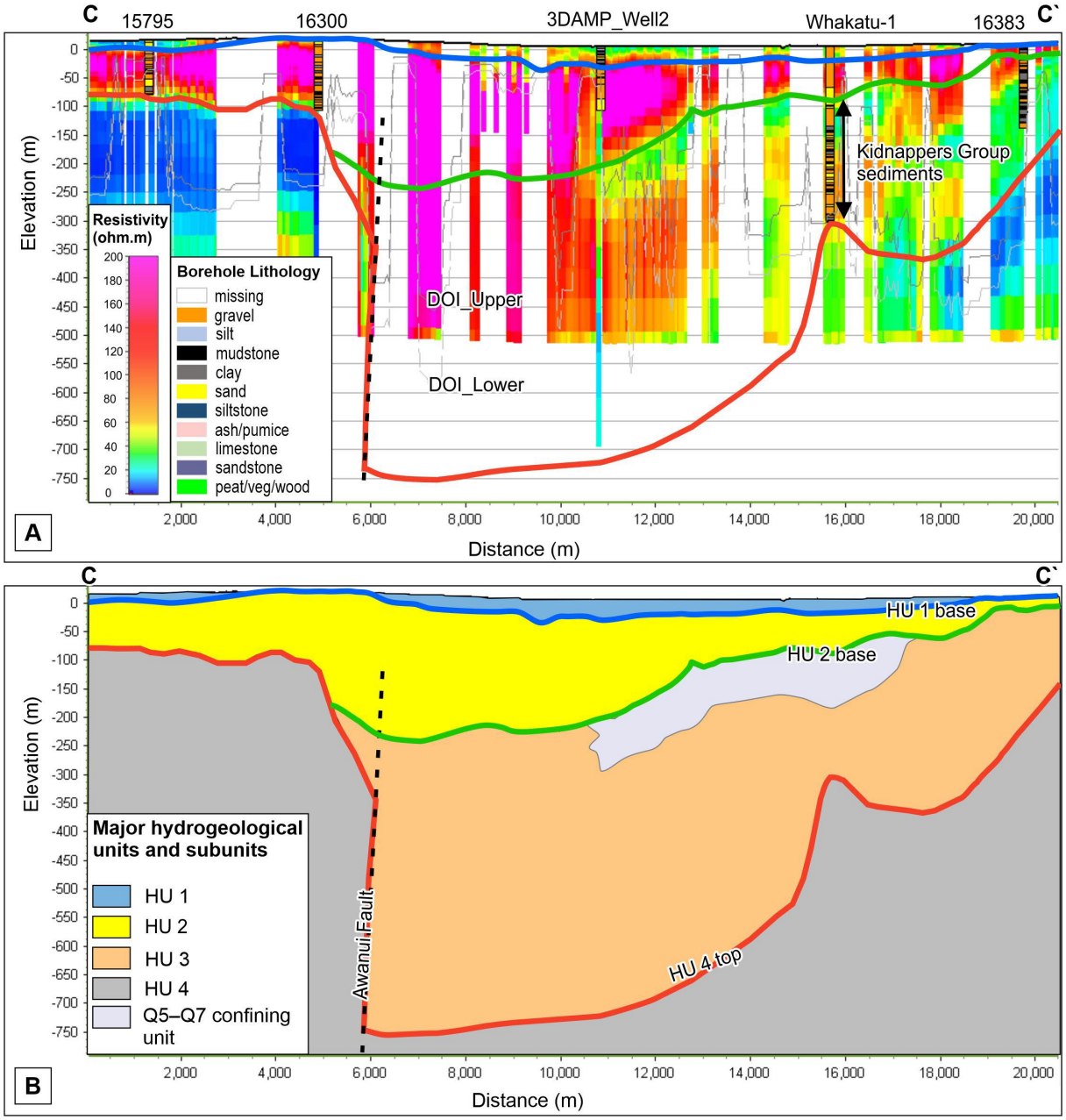


Figure 4.2 (A) NW–SE resistivity profile (C–C`; see location in Figure 2.1) across the study area showing the boundaries for each hydrogeological unit (HU). DOI_Lower and DOI_Upper are shown as grey dashed lines on the resistivity data. (B). Hydrogeological conceptual interpretation based on the boundaries delineated in (A). Note: the interpretation of the Q5–Q7 confining unit in Figure 4.1b is mainly conceptual; it is displayed as it assisted with the HU 2 base boundary delineation (see Table 3.2).

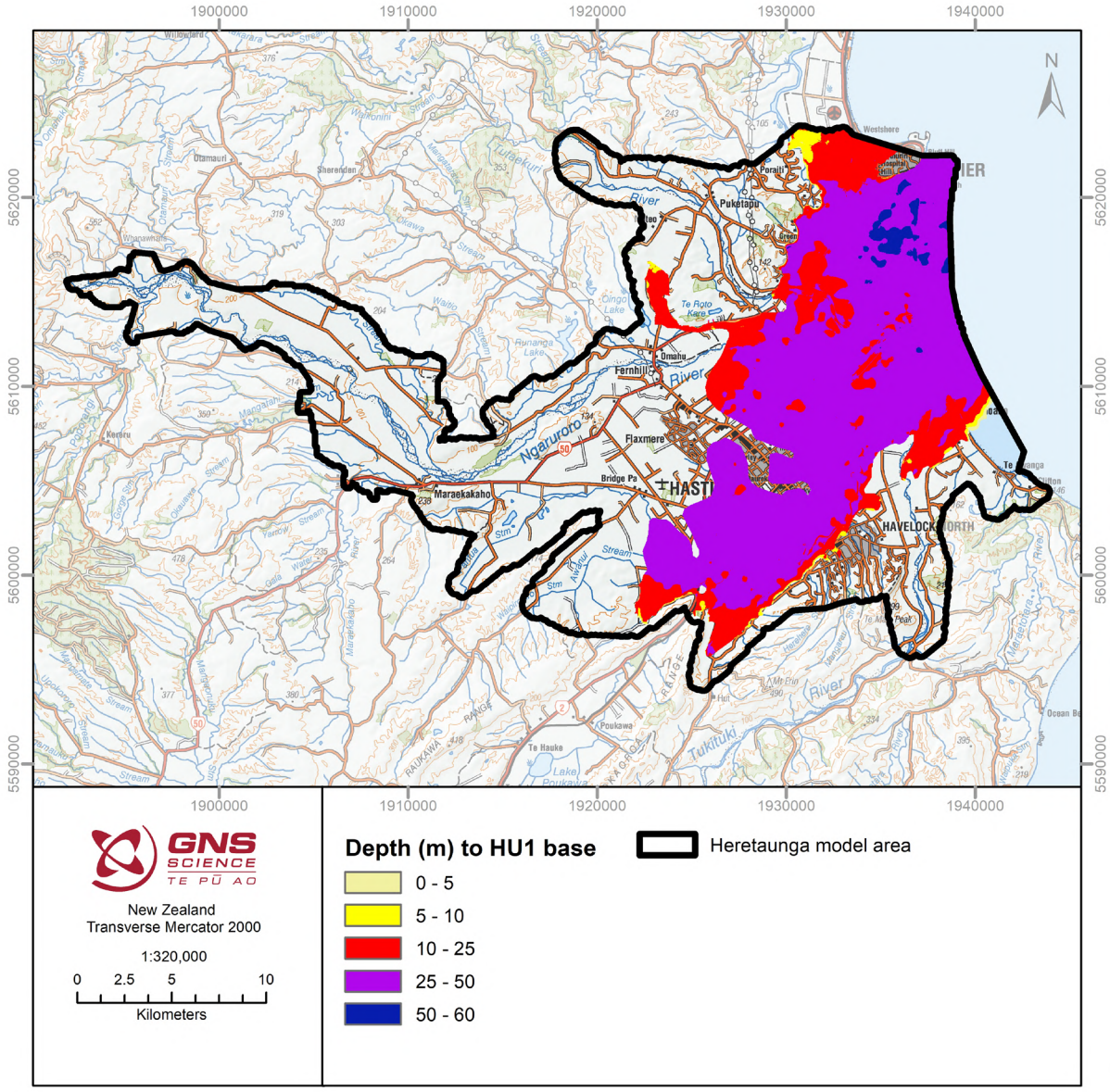


Figure 4.3 Map of depth to HU 1 base (confining layer).

## 4.2 HU 2 (Shallow Aquifer Unit)

HU 2 represents the second layer and shallower aquifer unit of this simple four-layer model of the aquifer system (Figure 4.1). The top of HU 2 is defined by the HU 1 base boundary where present, or the DEM where HU 1 is absent; the HU 2 base boundary is defined by the base of the primary high-resistivity group or by the HU 4 top boundary where these are coincident (Figure 4.1).

HU 2 shows two major resistivity groups: (1) high resistivity (>100 ohm.m) and (2) low to moderate resistivity (<40 and 40–100 ohm.m). Borehole data and surface geological maps suggest that the high-resistivity group is mainly composed of gravel-dominated lithologies ranging in age from Q1 to Q5 (Figure 4.1a). These gravel deposits primarily occur along depositional pathways of the Ngaruroro, Tutaekuri and Tukituki rivers (Figure 2.6; Figure 4.4). Based on borehole data, the material showing low resistivity (<40 ohm.m) in this unit is composed of clay-dominated lithology of Q1 deposits, and the material showing moderate resistivity is composed of mixed gravel and sand lithologies with minor clay of the Q1 deposits. This low- and moderate-resistivity group mainly occurs in drained swamp and marine terrace areas (Figure 2.6) close to the hills and in river valleys upstream of the plains (Figure 3.6).

In parts of the central area, the HU 2 base boundary is picked where there is a sharp drop in resistivity interpreted as a Q5–Q7 confining unit (Figures 4.1 and 4.2). In other parts of the central area, the resistivity contrast between HU 2 and HU 3 is gradational, and it is often difficult to clearly demarcate the base of HU 2 based only on the resistivity models. Research boreholes and petroleum wells provide lithological information on the deeper stratigraphy and hence provide some control points to demarcate the base of this layer in this area. This gradational resistivity between these layers could be related to the similar lithological composition and/or lower resolution of the SkyTEM resistivity models at greater depths. Therefore, the uncertainty in interpretation of the HU 2 base boundary in these areas is high.

As suggested in previous studies (Dravid and Brown 1997; Lee et al. 2014; Rakowski and Knowling 2018; Morgenstern et al. 2018), the high-resistivity part of the HU 2 is considered the main aquifer in the Heretaunga Plains due to its unconsolidated gravel-dominated lithology and highly transmissive character. This unit has been referred to as the Heretaunga aquifer (Rakowski and Knowling 2018; Morgenstern et al. 2018) and the Ngaruroro-Tutaekuri aquifer system (Dravid and Brown 1997) in previous studies. In comparison to previous models (Dravid and Brown 1997; Lee et al. 2014; Begg et al. 2022), HU 2 includes Q2–Q5 Last Glacial and interglacial riverbed gravel deposits (i.e. Maraekakaho Formation and part of Q5 deposits) and some river valley portions of the post-glacial Q1 deposits (parts of the high-resistivity Tollemache Member that do not overlie the Awatoto Member). The high-resistivity post-glacial Q1 deposits are laterally connected with the Q2–Q5 gravel deposits and are interpreted to be hydraulically connected (Figures 4.1 and 4.2). The low- to moderate-resistivity portion of the Q1 deposits falling outside the boundary of the confining unit (Figure 3.6) are considered to have low to moderate permeability due to its clay-silt-sand mixed lithology.

HU 2 deposits are distributed within the major river valleys upstream of the plains and in the central and eastern part of the SkyTEM survey area (Figures 4.4 and 4.5). The thickness of this layer is up to ~170 m along the Ngaruroro and Tutaekuri river valleys upstream from the plains and up to ~30 m along the Tukituki River (Figure 4.5). HU 2 is thicker along the paleo-Tutaekuri river compared to the current location of the river (~70 m at current Tutaekuri River). Most of HU 2 at the Tukituki River upstream of the plains has a thickness <5 m and sits directly over the basement rocks (HU 4). Thick river fan deposits (a maximum thickness of 295 m) from these rivers occur along a NE-trending graben in the central part of this survey area.

QMAP faults (Figure 2.4) suggest that the Awanui Fault primarily controls this NE-trending graben. Where HU 2 is exposed, it is considered to be an unconfined aquifer, and, where HU 2 is overlain by HU 1, HU 2 is considered to be a confined aquifer (Figure 3.6).

The maximum HU 2 depth of 295 m is deeper than the previous numerical groundwater model (250 m; Rakowski and Knowling 2018), suggesting that the depth of the groundwater model may need to be extended. In this area, the boundary between HU 2 and HU 3 is uncertain because HU 3 also has moderate to high resistivity through this area. Unfortunately, there are no boreholes in this area that extend to depths great enough to assess the permeability and water content of the material deeper than ~100 m (Figure 4.6). The deepest borehole in this area is the recently drilled 3DAMP_Well2 (Figure 4.6), which had to stop drilling at 114 m due to difficulties in drilling (slow penetration and budgetary constraints) through thick deposits of large-diameter gravels (Lawrence et al. 2021).

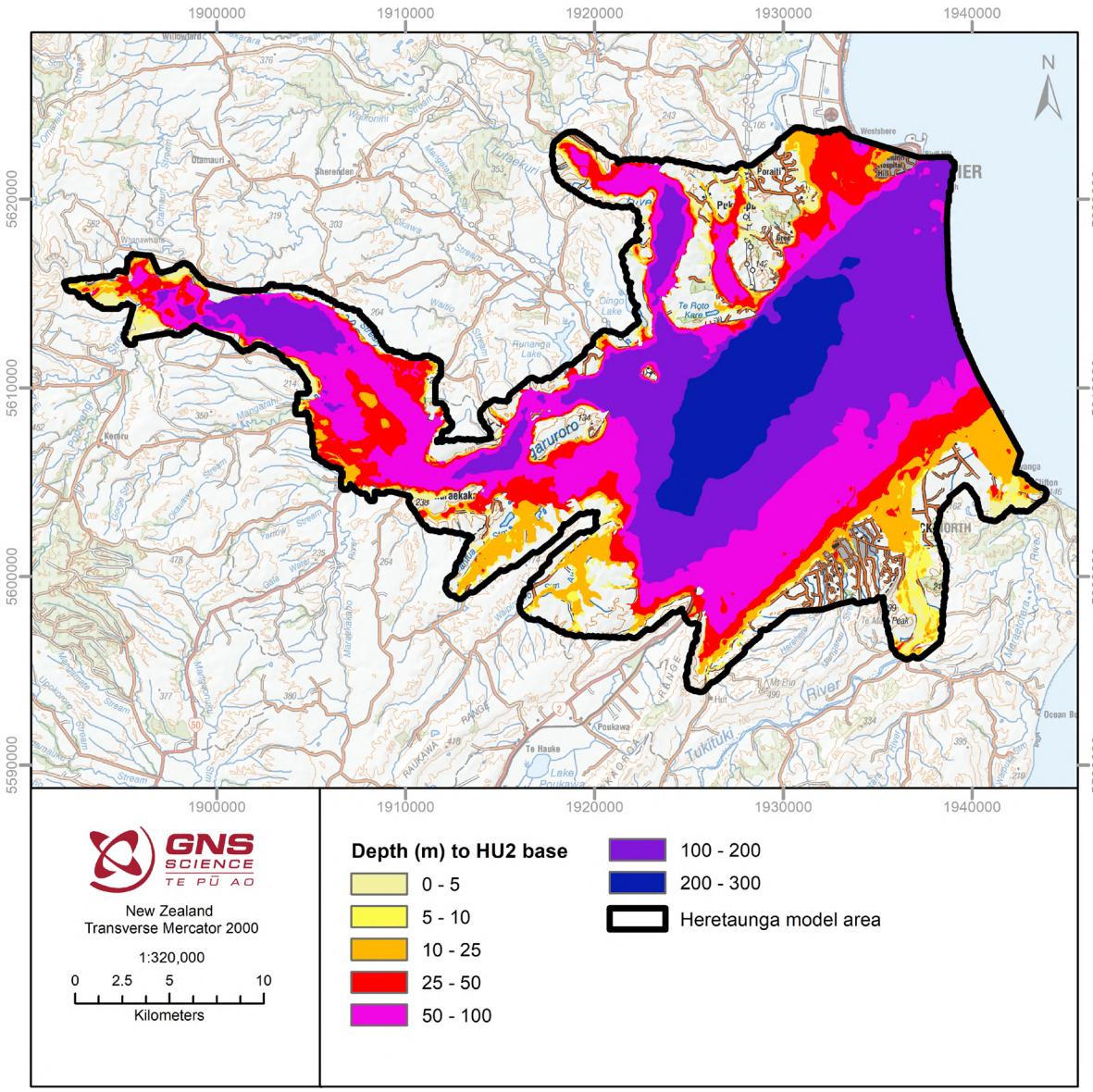


Figure 4.4 Map of depth to HU 2 base.

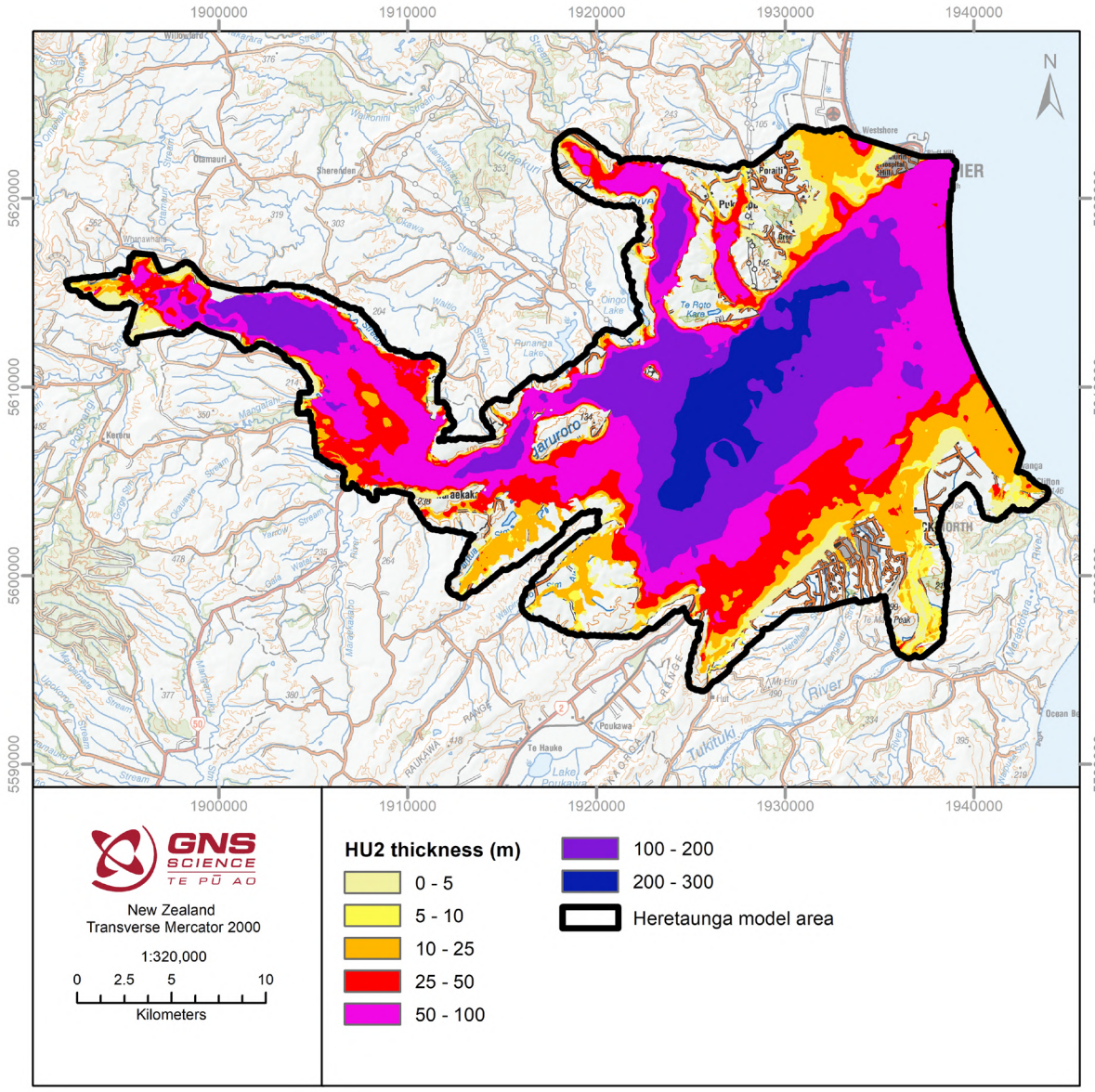


Figure 4.5 Thickness map of HU 2 (shallow aquifer unit).

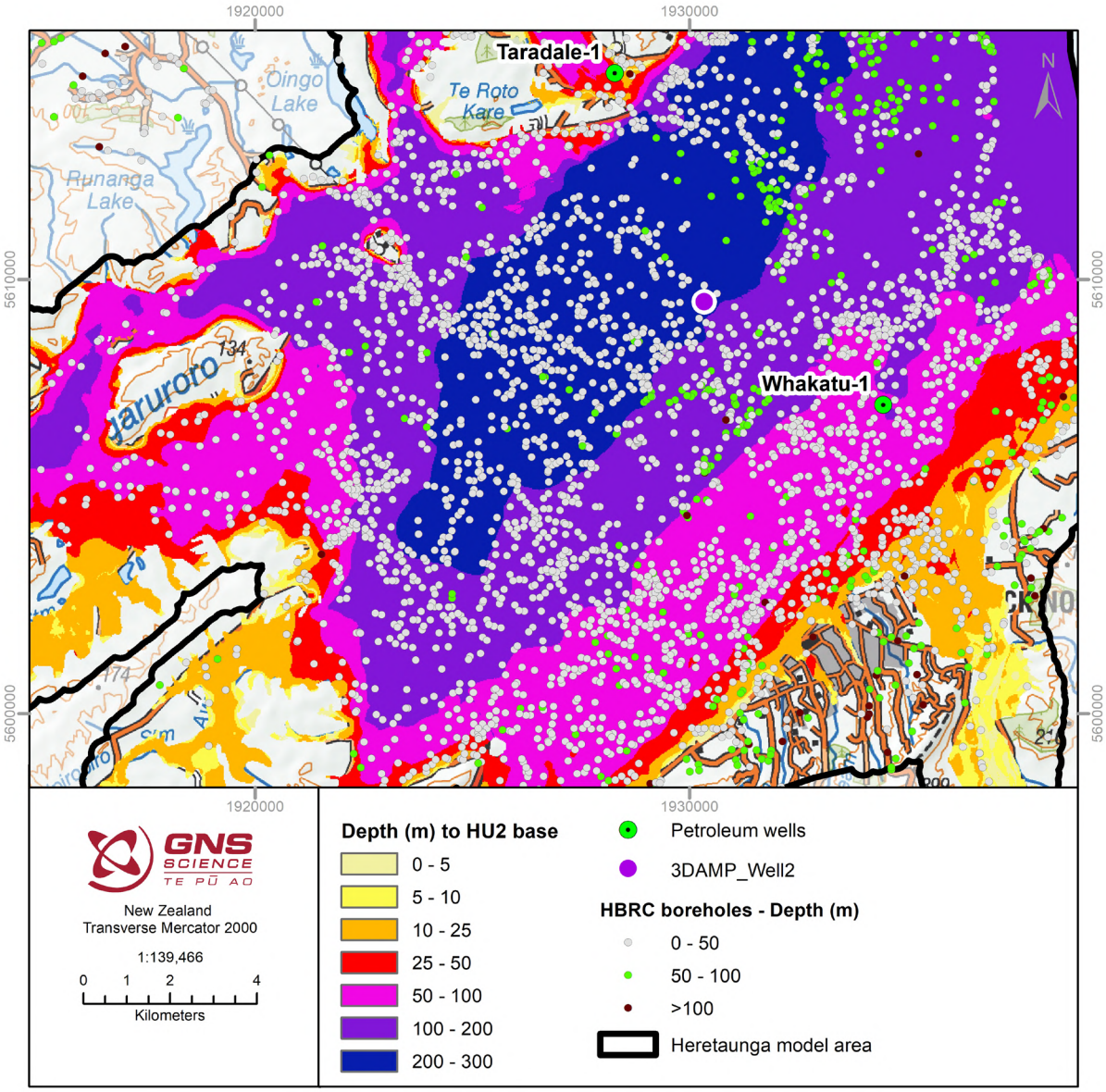


Figure 4.6 Zoom-in of the deepest mapped portion of the HU 2 base, compared with borehole depths in the area and the locations of petroleum wells and the recently drilled 3DAMP_Well2.

## 4.3 HU 3 (Deep Aquifer Unit)

HU 3 represents the third layer and the deep aquifer unit of this simple four-layer model of the aquifer system (Figure 4.1). The top of HU 3 is defined by the HU 2 base boundary where this exists, or the DEM where it does not, and the base of HU 3 is defined by the HU 4 top boundary (Figure 4.1).

HU 3 is a thick interval below HU 2 that includes layers of alternating low- and moderate- to high-resistivity groups of material. Due to limited well data, mapping of individual layers within this unit was not carried out in this simplified hydrogeological unit interpretation. In the eastern areas, low-resistivity groups (<40 ohm.m) are prominent features. In the western and central areas, HU 3 mainly shows moderate to high resistivity (40–120 ohm.m) and the boundary between HU 2 and HU 3 is more uncertain (see Section 4.2).

Deep borehole data (e.g. Whakatu-1, Flaxmere, Tollemache and Awatoto; Kellett et al. 2022) and surface geology (Lee et al. 2014, 2020) provide lithological information on HU 3. The low-resistivity groups are composed of fine-grained marine to marginal marine sediments that were deposited during the interglacial and penultimate interglacial climatic cycles (Q5–Q7, Middle to Late Pleistocene; Dravid and Brown 1997). The moderate-to high-resistivity groups (40–100 ohm.m) are widespread vertically and laterally (Figures 4.1–4.2) and were deposited during the Q5–Q7 interglacial and penultimate interglacial climatic cycles (Figure 4.1; Dravid and Brown 1997). In the southeastern areas close to the coast, HU 3 is exposed at the surface and represents beach gravels and sands (Figure 2.5; Brookfields Formation). Elsewhere, this unit is composed of alternating layers of gravel, sands and silt that were deposited as river and fan deposits. Some high-resistivity groups (>100 ohm.m) also occur in the central region of the SkyTEM survey area. There is no available borehole data that describes the lithology or age of these high-resistivity groups. However, based on correlation from the limited petroleum wells, they are considered to have been deposited mainly during Q5–Q7 (Dravid and Brown 1997). Based on a similar resistivity character as the overlying HU 2 and its location along the paleo riverbeds, these high-resistivity groups are interpreted to be composed of gravel-dominated lithology. The underlying moderate- to high-resistivity group (Figure 4.1) and the entirety of HU 3 at Whakatu-1 well (Figure 4.2) represent terrestrial to marginal marine deposits of Kidnappers Group and were deposited during the Early to Middle Pleistocene (Dravid and Brown 1997; Lee et al. 2014; Begg et al. 2022). Based on Whakatu-1 well lithology, these terrestrial and marginal marine groups are composed of alternating layers of gravel, sands and silt.

HU 3 includes both aquifers and aquitards and is expected to be more compacted than the overlying HU 2. Aquifers are coarse-grained river and fan deposits and beach deposits (Brookfields Formation) of Q5–Q7 and terrestrial to marginal marine coarse-grained deposits of Early to Middle Pleistocene Kidnappers Group. Aquitards are the Q5–Q7 fine-grained marine to marginal marine deposits. Resistivity data suggest that both aquifer and aquitard materials occur in the central and eastern areas, but, in the far western areas, HU 3 is dominated by aquifer material. In previous numerical groundwater modelling (Rakowski and Knowling 2018), the Q5–Q7 modelled geological units up to a depth of 250 m were used as a deep aquifer unit. Contrary to this model, we have also considered the Kidnappers Group as a deep aquifer unit due to the presence of moderate- to high-resistivity groups and gravel-dominated lithology in some areas.

HU 3 deposits have a maximum thickness of 616 m in the central region of the SkyTEM survey area and are mainly distributed on the eastern side of the Awanui Fault (Figures 2.4, 4.7 and 4.8). A thick graben developed in a NE trend parallel to the Awanui Fault (Figures 2.4 and 4.7). The displacement along this fault during the Early to Middle Pleistocene may have created the accommodation space for the HU 3 deposits.

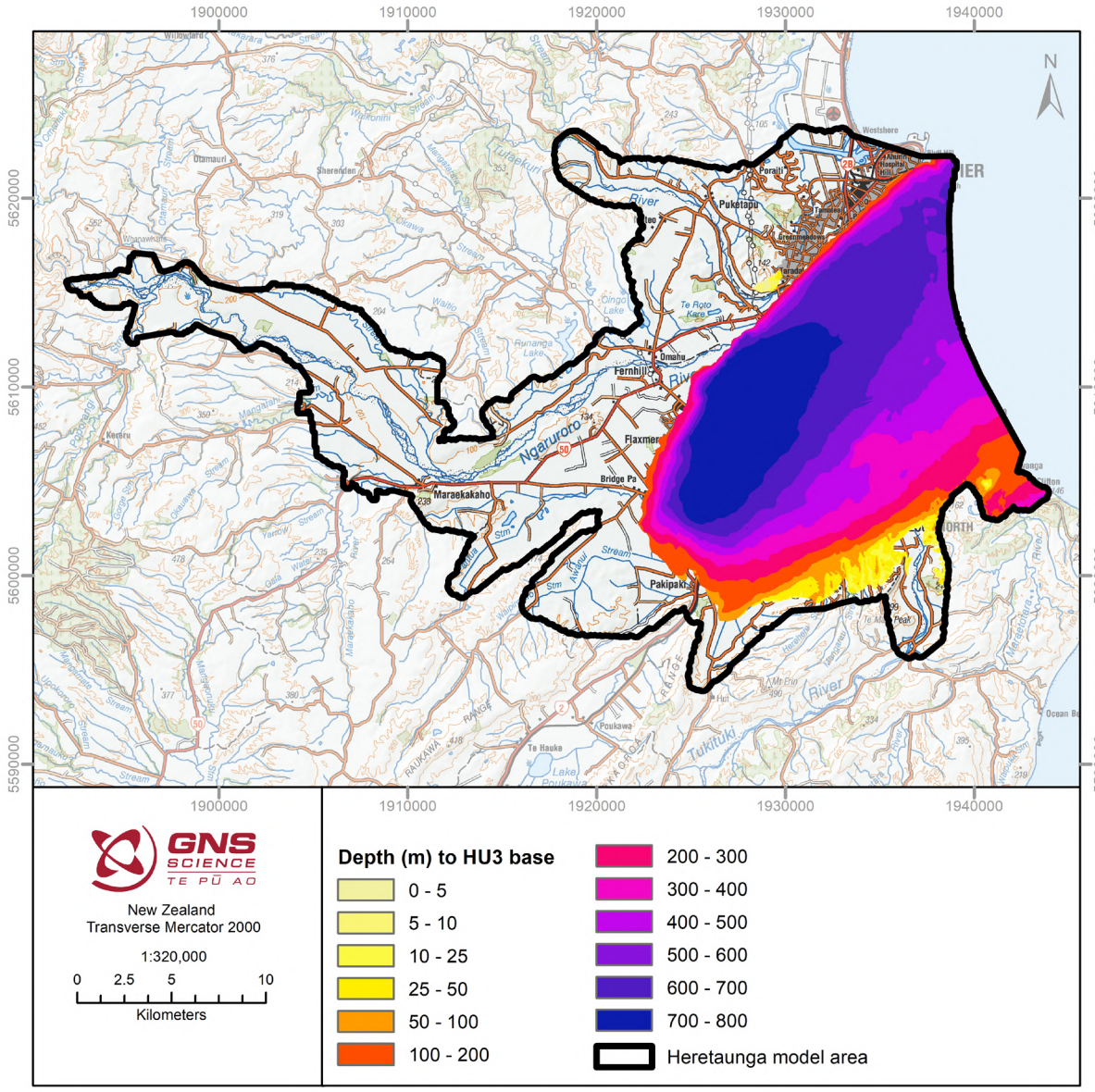


Figure 4.7 Depth to HU 3 base.

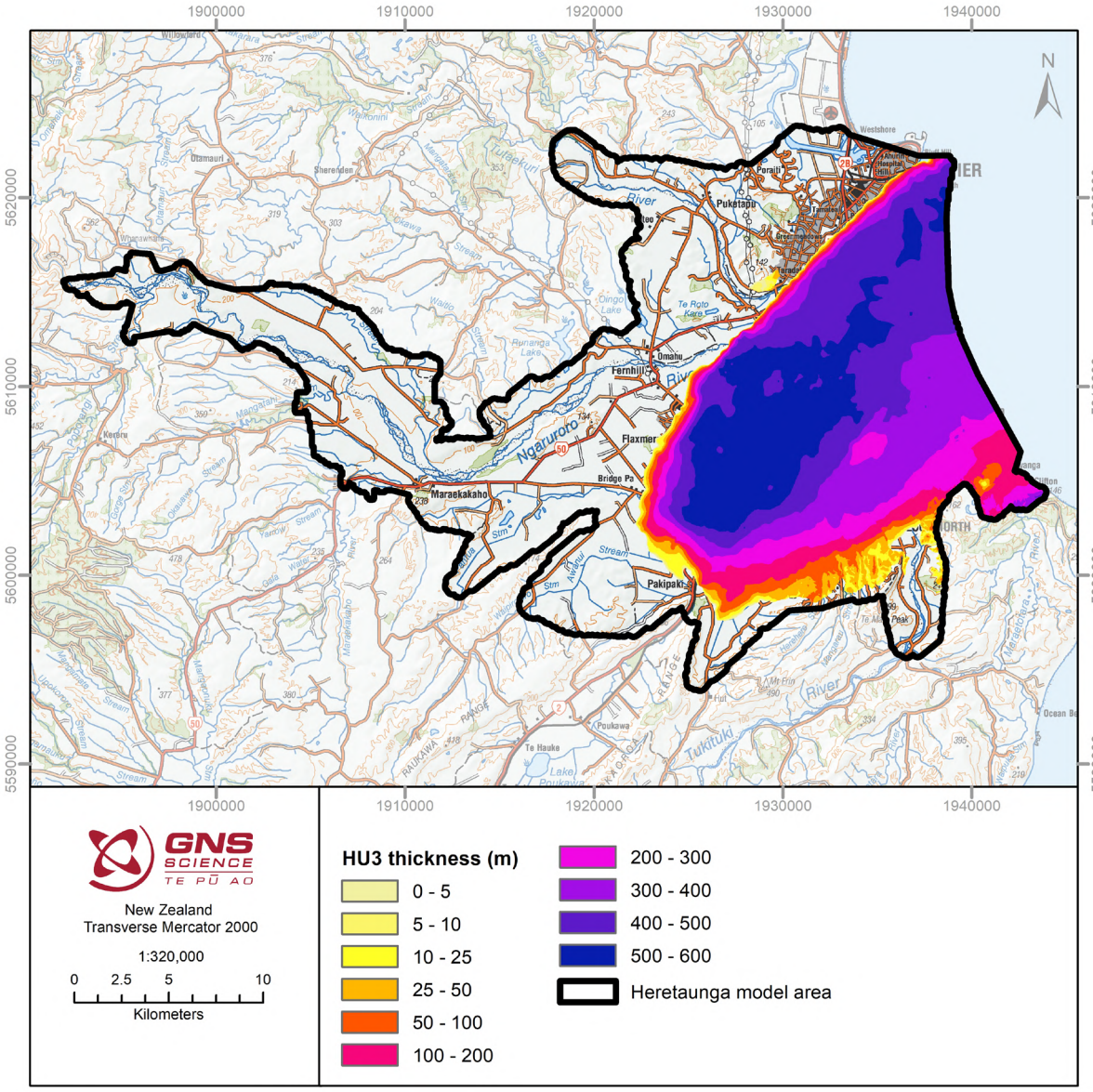


Figure 4.8 Thickness map of HU 3 (deep aquifer).

## 4.4 HU 4 (Basement Unit)

HU 4 represents the fourth layer and the basement unit of this simple four-layer model of the aquifer system (Figure 4.1). The HU 4 top boundary was defined as: the DEM elevation where basement is mapped as outcrop in the surface geological maps, or the top of the deep low-resistivity group, or where HU 4 top occurs below the extent of the resistivity models. Other information sources were utilised to define the HU 4 top boundary (Figure 4.1). These other information sources include seismic data (Tschritter et al. 2022), petroleum wells and previous geological model boundaries (top of Paleocene to Early Pleistocene model unit; Begg et al. 2022).

Pliocene and older sedimentary deposits are consolidated rocks and therefore considered to be the hydrogeological basement in this study. Surface geology suggests that HU 3 overlies the HU 4 basement rocks of Pliocene to Early Pleistocene Mangaheia Group sandstone, limestone and mudstone at the hills north, west and south of the Heretaunga Plains. To the southeast, basement rocks are Paleocene–Pliocene Mangatu, Tolaga and Mangaheia Group rocks composed mainly of mudstone, sandstone and limestone (see Figures 2.4 and 2.5 surface geology maps for details on the formation names and lithology).

HU 4 shows a variable resistivity character depending on the lithology. Throughout most of the area, HU 4 is composed of siliciclastic rocks and has low resistivity values (<40 ohm.m). In areas where HU 4 is composed of limestones, it has high resistivity values (>100 ohm.m). Limestone is utilised for groundwater resources around the boundaries of the Heretaunga Plains; however, these resources are not typically modelled as part of the main unconsolidated aquifer and are therefore included within the HU 4 basement unit. Basement rocks encountered at petroleum wells are limited (at 307 m depth, base Kidnappers Group at Whakatu-1; ~42.7 m at Taradale-1; 8.5 m at Hukarere-1 drillhole; Tschritter et al. 2022). In the central region, HU 4 top goes below the SkyTEM data depth.

Figure 4.9 depicts the depth to basement (depth to HU 4 top boundary), which varies from 0 to 800 m through the Heretaunga model area. The deepest portion of the model occurs in the central plains, coincident with the deepest portions of HU 2 and HU 3.

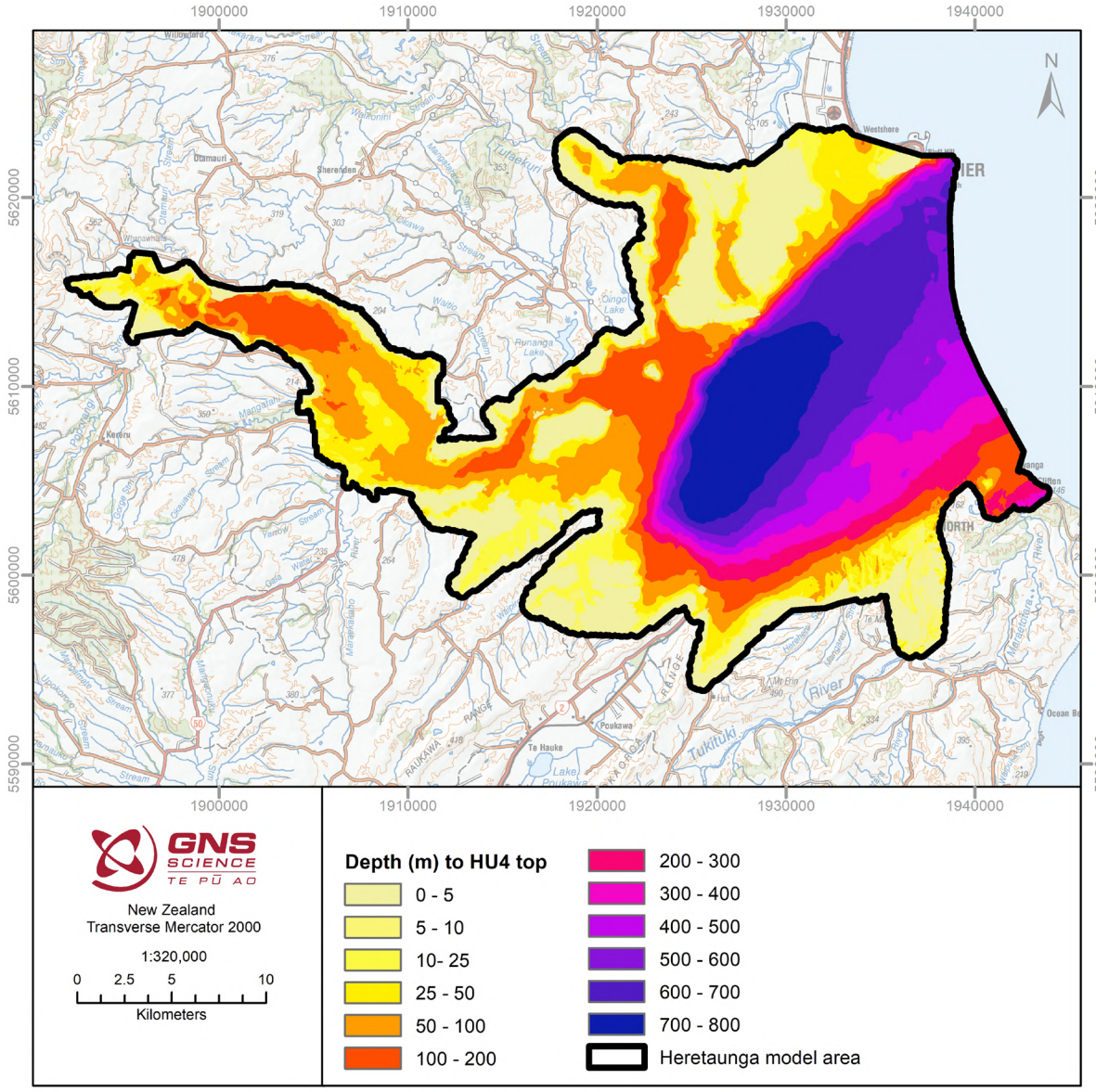


Figure 4.9 Depth to HU 4 top (depth to basement).

## 4.5 Offshore Extension of Hydrogeological Units

The extension of the aquifer system offshore has been suggested by previous seismic data interpretations in Hawke Bay (Paquet et al. 2009, 2011; Mountjoy 2019) and a previous groundwater study (Dravid and Brown 1997). The variations in resistivity in offshore SkyTEM data also indicate the extension of onshore HUs in the offshore area. However, the mapping of HU boundaries is more challenging offshore compared to the onshore area due to (1) depth limitation of the SkyTEM data and (2) influence of saline water on resistivity.

The extremely low resistivity of sea water impacts how deep the SkyTEM system can penetrate, and in the smooth offshore model, for example, the standard depth of investigation varies from 20 m to 72 m and the data penetration limit is 100 m below sea level (Section 2.1; Figure 2.2). As the bulk resistivity measured by SkyTEM is sensitive to the resistivity of pore water, near-surface infiltration of saline water is likely to reduce the bulk resistivity of offshore aquifers compared to onshore. Throughout the Heretaunga Plains, groundwaters have resistivities of 14.1–85.1 ohm.m (Tschritter et al. 2022). At the base of the sea water column, the resistivity models display a transition zone from very low saline resistivities (0.2–0.3 ohm.m) to resistivities that indicate some freshwater saturation (>8.3 ohm.m). This near-surface infiltration of saline water results in bulk resistivity values that are not comparable between the onshore and offshore portions of data, particularly in the seabed portion of the models that likely correspond to the offshore extension of HU 1. Therefore, relative changes in resistivity at depth within the offshore resistivity models are considered of more importance than absolute values of resistivity for the mapping of HU boundaries.

In this study, we have extrapolated the hydrogeological unit boundaries in the offshore region, taking control points from the onshore areas and continuing the general trend observed within the onshore area, considering any marked relative changes in resistivity (Figure 4.10). In general, the HU 1 shows low resistivity <8 ohm.m and the HU 2 shows ~8–70 ohm.m resistivity in the offshore resistivity data. As suggested in the Venice system for classification of marine waters (Madarasz-Smith et al. 2016), the <8 ohm.m resistivity units are considered to be highly influenced by saline water. The resistivity in the river-mouth areas is relatively high compared to the other offshore regions (Figure 4.10a). This may be due to higher freshwater recharge in the river-mouth areas that cause elevated resistivity compared to other regions.

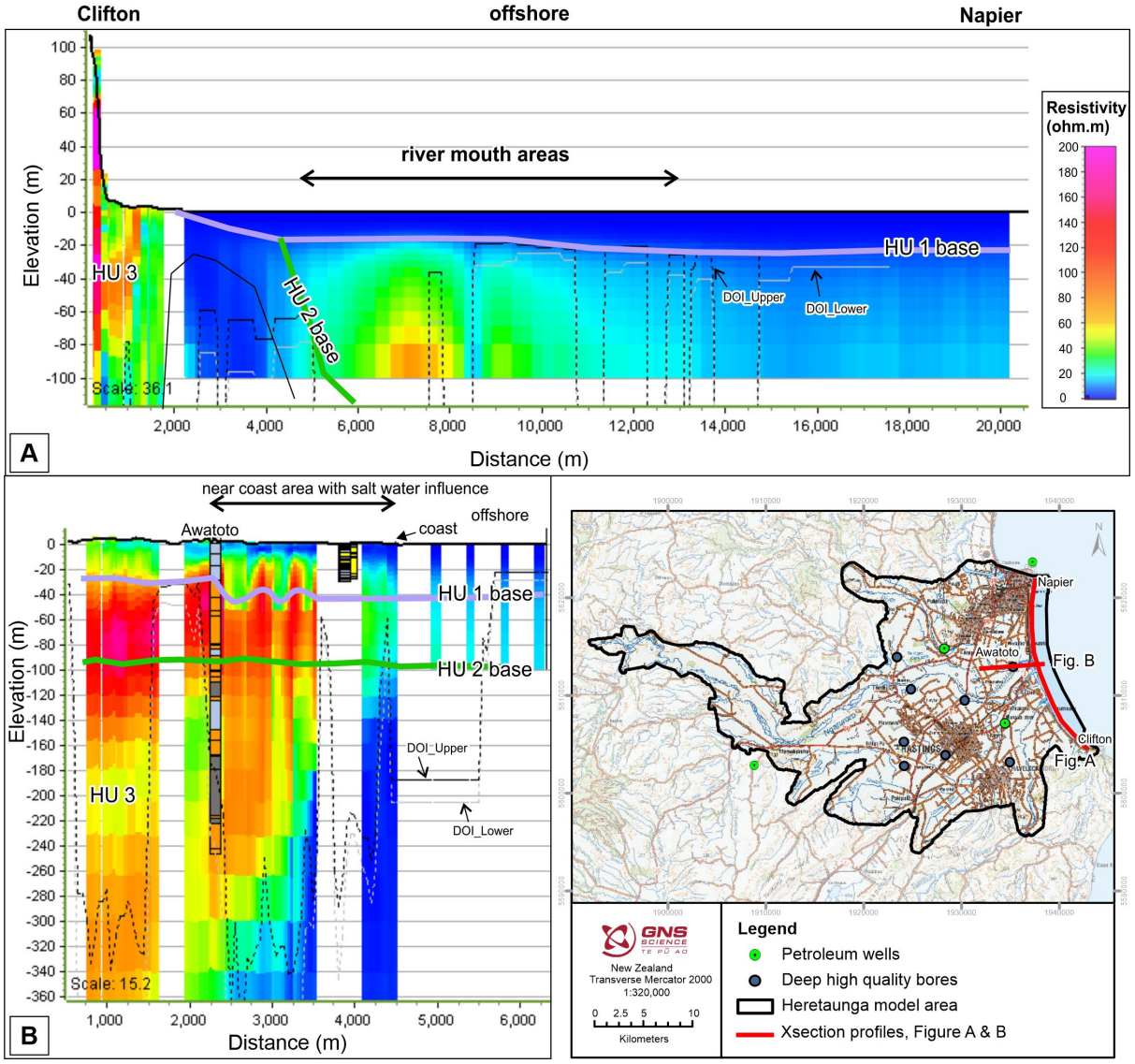


Figure 4.10 (A) Offshore SkyTEM (smooth) resistivity profile from Clifton to Napier. (B) East–west SkyTEM (smooth) resistivity profile from near-coast areas to offshore. DOI_Lower and DOI_Upper are shown as grey dashed lines on the resistivity data in (A) and (B).

# 5.0 DIGITAL DELIVERABLES

All data are geo-referenced to the New Zealand Transverse Mercator (NZTM 2000) coordinate system and New Zealand Vertical Datum 2020 (NZVD2016).

## 5.1 Primary Datasets

The primary datasets delivered are the boundary surfaces, which are delivered in the readily accessible ascii grid format (with 25 m resolution):

- *Surfaces\HU1_base_V1_2022.asc*
- *Surfaces\HU2_base_V1_2022.asc*
- *Surfaces\HU4_top_V1_2022.asc*

The top of the hydrogeological model is provided by a 25 m DEM (see Section 2.2.2).

- *Surfaces\HeretaungaSkyTEM_DEM_25m.asc*

## 5.2 Supplementary Datasets

Additional datasets are provided that were utilised in the construction of the primary datasets.

Manual interpretation points that were used to generate the surfaces are provided as x,y,z *.csv files:

- *Points\HU1_base_points_V1_2022.csv*
- *Points\HU2_base_points_V1_2022.csv*
- *Points\HU4_top_points_V1_2022.csv*

Polygons utilised for refinement of the surfaces at the ground surface are provided as shapefiles (see Section 3.2):

- *Polygons\Heretaunga_ArtesianConditions_V1_2022.shp*
- *Polygons\Heretaunga_GeoMap_SedimentsOverlyingBasement.shp*
- *Polygons\Heretaunga_GeoMap_EarlyPleistocenetoQ5.shp*
- *Polygons\Heretaunga_GeoMap_InternalBasement.shp*

# 6.0 CONCLUSIONS AND RECOMMENDATIONS

This report focuses on the mapping of major hydrogeological units that correspond to the large-scale hydrogeological characteristics of the SkyTEM-derived resistivity models in the Heretaunga Plains as part of the Hawke's Bay 3D Aquifer Mapping Project (3DAMP).

Using the SkyTEM-derived resistivity models and supporting information, a simple four-layer hydrogeological model was created for the Heretaunga model area that consists of:

- HU 1 (confining unit)
- HU 2 (shallow aquifer unit)
- HU 3 (deep aquifer unit)
- HU 4 (basement unit).

This four-layer model was defined by the DEM and the manually delineated boundaries:

1. HU 1 base
2. HU 2 base
3. HU 4 top.

HU 1 (Q1 deposits) forms the major confining unit in the area and exhibits a low- to moderate-resistivity signature. This HU includes the clay-silt-dominated lithology of the Awatoto Member and the overlying lithologies of the Tollemache Member of the Heretaunga Formation.

HU 2 (Q1–Q5 deposits) forms the shallow aquifer unit in the area and mainly exhibits a high-resistivity signature, with some minor areas of low to moderate resistivity. This HU includes the Maraekakaho Formation (Last Glacial gravels) and all terrestrial sediments of the Heretaunga Formation (Tollemache Member) that do not overlie the clay-silt-dominated sediments of the Awatoto Member, as well as Q5 sediments with a moderate- to high-resistivity signature.

HU 3 (Early to Middle Pleistocene deposits, including Q5–Q7 deposits) forms a deeper aquifer unit that consists of alternating layers of low and high resistivity, which are interpreted to be alternating aquifer and aquitard materials. This HU includes the penultimate glacial gravels; and last and penultimate interglacial, Brookfields Formation and Kidnappers Group sediments.

HU 4 (Paleocene to Early Pleistocene deposits) forms the hydrogeological basement unit and primarily exhibits a low-resistivity signature. This HU includes various consolidated rock formations. Some groundwater resources are present within the limestone-dominated areas of the Mangaheia group, which exhibit a high-resistivity signature.

Uncertainties are present in the resistivity models and manually delineated major hydrogeological units. However, the datasets from this study enable a 3D view of the subsurface hydrogeology of the entire survey area not previously possible. Distributions of the hydrogeological units are largely consistent with the existing understanding of groundwater resources in the Heretaunga Plains, with additional refinements of the confining and shallow aquifer layers. SkyTEM data in this study also provides better mapping of the deep aquifer and hydrogeological basement in the region.

The gridded surfaces of the boundaries between the major hydrogeological units provide valuable information that will be utilised within subsequent interpretation and modelling work as part of 3DAMP.

**Recommendations**

- The maximum HU 2 depth of 295 m is deeper than the previous numerical groundwater model (250 m), suggesting that the depth of the groundwater model may need to be extended.
- Additional drilling through the deepest area of HU 2 and HU 3, where a medium- to high-resistivity signature extends to the base of the SkyTEM-derived resistivity models, would be advantageous for determining groundwater model boundary conditions and hydraulic conductivity through this region at depth. Due to previous complications encountered with drilling (3DAMP_Well2; Lawrence et al. 2021), a larger drilling rig designed to penetrate to intermediate or deep depths would be needed (rather than a standard groundwater drilling rig).

Smaller areas could be studied in more detail to undertake fault delineation and refine relationships between the resistivity values and the local materials.

## 7.0 ACKNOWLEDGEMENTS

This work has been jointly funded by the New Zealand Government's Provincial Growth Fund, Hawke's Bay Regional Council and GNS Science's Strategic Science Investment Fund (Ministry of Business, Innovation & Employment).

Thank you to Jeff Smith and Simon Harper of Hawke's Bay Regional Council for their contributions to this project. Thank you to Amanda Langley of Project Haus for project management support.

Thank you to Chris Worts for business partnerships support. We thank Julie Lee for her input in various technical discussions and for providing high-resolution pictures of surface geology and stratigraphy in the Napier-Hastings urban area. Thank you to Conny Tschritter and Matthew Coble for providing report reviews.

## 8.0 REFERENCES

Auken E, Christiansen AV, Kirkegaard C, Fiandaca G, Schamper C, Behroozmand AA, Binley A, Nielsen E, Effersø F, Christensen NB, et al. 2015. An overview of a highly versatile forward and stable inverse algorithm for airborne, ground-based and borehole electromagnetic and electric data. *Exploration Geophysics*. 46(3):223–235. doi:10.1071/EG13097.

Auken E, Christiansen AV, Westergaard JH, Kirkegaard C, Foged N, Viezzoli A. 2009. An integrated processing scheme for high-resolution airborne electromagnetic surveys, the SkyTEM system. *Exploration Geophysics*. 40(2):184–192. doi:10.1071/EG08128.

Begg JG, Jones KE, Lee JM, Tschritter C. 2022. 3D geological model of the Napier-Hastings urban area [explanatory text]. 21 p. Lower Hutt (NZ): GNS Science. (GNS Science geological map; 7b). doi:10.21420/QFEK-9369.

Dravid PN, Brown LJ. 1997. Heretaunga Plains groundwater study. Volume 1: findings. Napier (NZ): Hawke's Bay Regional Council. 238 p.

Farrier T. 2020. 3D Aquifier Mapping Project DEM Version 2. Napier (NZ): Hawke's Bay Regional Council.

Hemmings B. 2022. Personal communication. Groundwater Modeller, Groundwater Modelling; GNS Science, Wairakei, NZ.

Heron DW, custodian. 2020. Geological map of New Zealand [map]. 3rd ed. Lower Hutt (NZ): GNS Science. 1 USB, scale 1:250,000. (GNS Science geological map; 1).

Kellett RL, Rawlinson ZJ, Griffin AG, Lawrence MJF, Tschritter C, Sahoo TR, Herpe M. 2022. Hawke's Bay 3D Aquifer Mapping Project: deep borehole interpretation within Heretaunga Plains in the context of SkyTEM data and new Borehole 17137 (3DAMP_Well2). Lower Hutt (NZ): GNS Science. 44 p. Consultancy Report 2022/90. Prepared for Hawke's Bay Regional Council.

Lawrence MJF, Kellett RL, Pradel GJ, Sanders F, Herpe M, Rawlinson ZJ, Reeves RR, Brakenrig T, Moreau M, Cameron SG, et al. 2021. Hawke's Bay 3D Aquifer Mapping Project: drilling completion report for Borehole 17137 (3DAMP_Well2), Morley Road, Heretaunga Plains. Lower Hutt (NZ): GNS Science. 90 p. Consultancy Report 2021/40. Prepared for Hawke's Bay Regional Council.

Lee JM. 2021 Nov. Personal communication. Geologist, Geological Mapping & Stratigraphy; GNS Science, Lower Hutt, NZ.

Lee JM, Begg JG, Bland KJ. 2020. Geological map of the Napier-Hastings urban area [map]. Lower Hutt (NZ): GNS Science. 1 map, scale 1:75,000. (GNS Science geological map; 7a).

Lee JM, Begg JG, Townsend DB. In prep. Geomorphological map of the Napier-Hastings urban area. Scale 1:50,000. Lower Hutt (NZ): GNS Science. (GNS Science geological map; 7c).

Lee JM, Bland KJ, Townsend DB, Kamp PJJ. 2011. Geology of the Hawke's Bay area [map]. Lower Hutt (NZ): GNS Science. 1 folded map + 93 p., scale 1:250,000. (Institute of Geological & Nuclear Sciences 1:250,000 geological map; 8).

Lee JM, Tschritter C, Begg JG. 2014. A 3D geological model of the Greater Heretaunga/Ahuriri Groundwater Management Zone, Hawke's Bay. Lower Hutt (NZ): GNS Science. 31 p. Consultancy Report 2014/89. Prepared for Hawke's Bay Regional Council. https://www.hbrc.govt.nz/assets/Document-Library/Publications-Database/4814-RM16-28-Simplified-geological-model-for-the-Heretaunga-Plains-Ahuriri-GW-Mngt-June2014.pdf

Litchfield NJ. 2003. Maps, stratigraphic logs, and age control data for river terraces in the eastern North Island. Lower Hutt (NZ): Institute of Geological & Nuclear Sciences. 102 p. (Institute of Geological & Nuclear Sciences science report; 2003/31).

Madarasz-Smith A, Wade O, Wade H, Hicks A. 2016. The estuaries of the TANK catchments: Ahuriri and Waitangi estuaries, values, state and trends. Napier (NZ): Hawke's Bay Regional Council. 118 p. HBRC Report RM 16-20.

Morgenstern U, Begg JG, van der Raaij RW, Moreau M, Martindale H, Daughney CJ, Franzblau RE, Stewart MK, Knowling MJ, Toews MW, et al. 2018. Heretaunga Plains aquifers: groundwater dynamics, source and hydrochemical processes as inferred from age, chemistry, and stable isotope tracer data. Lower Hutt (NZ): GNS Science. 82 p. (GNS Science report; 2017/33). doi:10.21420/G2Q92G.

Mountjoy JJ. 2019. Offshore framework of the Heretaunga Aquifer in Hawke Bay: a desktop study into the likely offshore extent of freshwater aquifers in Hawke's Bay and the relationship to mapped seeps. Wellington (NZ): National Institute of Water & Atmospheric Research. 20 p. Client Report 2019058WN. Prepared for Hawke's Bay Regional Council.

Paquet F, Proust J-N, Barnes PM, Pettinga JR. 2009. Inner-forearc sequence architecture in response to climatic and tectonic forcing since 150 ka: Hawke's Bay, New Zealand. *Journal of Sedimentary Research*. 79(3):97–124. doi:10.2110/jsr.2009.019.

Paquet F, Proust J-N, Barnes PM, Pettinga JR. 2011. Controls on active forearc basin stratigraphy and sediment fluxes: the Pleistocene of Hawke Bay, New Zealand. *Geological Society of America Bulletin*. 123(5–6):1074–1096. doi:10.1130/b30243.1.

Rakowski P, Knowling MJ. 2018. Heretaunga aquifer groundwater model: development report. Napier (NZ): Hawke's Bay Regional Council. 182 p. HRBC Report RM18-14.

Rawlinson Z. 2013. A review of the most effectual and economical geophysical techniques for characterising groundwater within New Zealand. Lower Hutt (NZ): GNS Science. 90 p. (GNS Science report; 2013/38).

Rawlinson ZJ, Foged N, Westerhoff RS, Kellet RL. 2021. Hawke's Bay 3D Aquifer Mapping Project: Heretaunga Plains SkyTEM data processing and resistivity models. Wairakei (NZ): GNS Science. 90 p. Consultancy Report 2021/93. Prepared for Hawke's Bay Regional Council.

Reeves RR, Rawlinson ZJ, Brakenrig T, Macdonald N. 2019. SkyTEM for groundwater knowledge refinement in the Heretaunga and Ruataniwha Plains: stage 2 – preliminary Transient Electro-Magnetic (TEM) soundings. Wairakei (NZ): GNS Science. 44 p. Consultancy Report 2019/77. Prepared for Hawke's Bay Regional Council.

SkyTEM Australia Pty Ltd. [2020]. Acquisition and processing report: SkyTEM helicopter EM survey, Hawkes Bay, NZ. Malaga (AU): SkyTEM Australia Pty Ltd. 33 p. Report AUS 10056. Prepared for Hawke's Bay Regional Council.

Sørensen KI, Auken E. 2004. SkyTEM – a new high-resolution helicopter transient electromagnetic system. *Exploration Geophysics*. 35(3):194–202. doi:10.1071/EG04194.

Tschritter C, Kellett RL, Rawlinson ZJ, Griffin AG. 2022. Hawke’s Bay 3D Aquifer Mapping Project: Heretaunga Plains data and model inventory. Wairakei (NZ): GNS Science. 96 p. Consultancy Report 2021/113. Prepared for Hawke's Bay Regional Council.


www.gns.cri.nz

**Principal Location**

1 Fairway Drive, Avalon
Lower Hutt 5010
PO Box 30368
Lower Hutt 5040
New Zealand
T +64-4-570 1444
F +64-4-570 4600

**Other Locations**

Dunedin Research Centre
764 Cumberland Street
Private Bag 1930
Dunedin 9054
New Zealand
T +64-3-477 4050
F +64-3-477 5232

Wairakei Research Centre
114 Karetoto Road
Private Bag 2000
Taupo 3352
New Zealand
T +64-7-374 8211
F +64-7-374 8199

National Isotope Centre
30 Gracefield Road
PO Box 30368
Lower Hutt 5040
New Zealand
T +64-4-570 1444
F +64-4-570 4657